NACA RM L9C31

NACA

RESEARCH MEMORANDUM

LONGITUDINAL STABILITY AND CONTROL CHARACTERISTICS OF A SEMISPAN WIND-TUNNEL MODEL OF A TAILLESS AIRPLANE AND A COMPARISON WITH COMPLETE-MODEL WIND-TUNNEL TESTS AND SEMISPAN-MODEL WING-FLOW TESTS

By Kenneth W. Goodson and Thomas J. King, Jr.

Langley Aeronautical Laboratory
Langley Air Force Base, Va.

NATIONAL ADVISORY COMMITTEE FOR AERONAUTICS

WASHINGTON

October 10, 1949
December March 26, 1956.

NACA RM L9C31

NATIONAL ADVISORY COMMITTEE FOR AERONAUTICS

RESEARCH MEMORANDUM

LONGITUDINAL STABILITY AND CONTROL CHARACTERISTICS OF A SEMISPAN WIND-TUNNEL MODEL OF A TAILLESS AIRPLANE AND A COMPARISON WITH COMPLETE-MODEL WIND-TUNNEL TESTS AND SEMISPAN-MODEL WING-FLOW TESTS

By Kenneth W. Goodson and Thomas J. King, Jr.

SUMMARY

An investigation was conducted on a semispan model of a tailless airplane in the Langley high-speed 7- by 10-foot tunnel in the Mach number range from 0.40 to 0.97. The results are compared with those obtained with a sting-mounted complete model tested in the same tunnel and with a semispan model tested by the wing-flow method.

The lift-curve slopes obtained for the semispan model and the wing-flow model were in good agreement but both were generally lower than the values obtained for the sting model. The results of an unpublished investigation have shown that tunnel-wall boundary-layer and strut-leakage effects can cause the difference noted between the lift-curve slopes of the sting and the semispan data.

Fair agreement was obtained among the data of the three models as regards the variation of pitching-moment coefficients with lift coefficient for various elevator deflections. In the Mach number range between 0.94 and 0.97, control reversal was indicated in the wing-flow data near zero lift; whereas, these same trends were indicated in the larger scale semispan data at somewhat higher lift coefficients.

All three test methods indicated a stable variation of control deflection with Mach number up to a Mach number of about 0.87 at an altitude of 30,000 feet and for a wing loading of 28. At higher Mach numbers all three methods also indicated a tucking-under tendency of similar abruptness and magnitude.

Tests of a 10-percent-span spoiler located on the 35-percent-chord line of the lower wing surface inboard of the vertical tail was equivalent to about 4° of negative control deflection in the high-speed range

where trim changes were encountered and, therefore, might be desirable for use as a means of auxiliary control.

INTRODUCTION

A number of investigations have been conducted at high subsonic and transonic Mach numbers with various models of a tailless airplane. Data have been obtained on a complete model mounted on a sting support in the Langley high-speed 7- by 10-foot tunnel (reference 1) and on a semispan model utilizing the NACA wing-flow method (unpublished). In order to obtain data at higher Mach numbers than were reached with the sting-supported model, one-half of this model was tested as a reflection-plane model in the Langley high-speed 7- by 10-foot tunnel. The purpose of this paper is to present these data and to compare the results with those obtained by other methods.

COEFFICIENTS AND SYMBOLS

The system of axes used for the presentation of the data, together with an indication of the positive forces, moments, and angles, is presented in figure 1. Pertinent symbols are defined as follows:

C_L lift coefficient (Lift/qS)

C_D drag coefficient (Drag/qS)

C_m pitching-moment coefficient, measured about 17-percent mean aerodynamic chord (Pitching moment/qSc')

Lift = -Z

Drag = -X (only at $\psi = 0^\circ$)

X force along X-axis, pounds

Z force along Z-axis, pounds

M pitching moment, pound-feet

q free-stream dynamic pressure, pounds per square foot ($\rho V^2/2$)

ρ mass density of air, slugs per cubic foot

V free-stream velocity, feet per second

M	free-stream Mach number (V/a)
a	speed of sound, feet per second
S	wing area (3.174 sq ft on complete model)
c'	mean aerodynamic chord (1.046 ft on model)
a.c.	aerodynamic center
c	chord parallel to plane of symmetry
c_l	chord perpendicular to 0.25c line
α	angle of attack, measured from X-axis to fuselage center line, degrees
R	Reynolds number ($\rho Vc'/\mu$)
μ	absolute viscosity of air, pounds-second/feet^2
δ_a	control-surface deflection with reference to wing chord line parallel to plane of symmetry, degrees

MODELS AND APPARATUS

A semispan model of a tailless airplane was used to obtain the basic semispan data presented in this paper. The model was made by utilizing one-half of a complete model (reference 1). However, inasmuch as the original fuselage was of solid steel construction, a half-fuselage was cast of bismuth-tin alloy for use in these tests. The control surfaces were of constant chord with sealed gaps. Drawings and photographs of the model are presented in figures 2 to 4. Details of a 10-percent-span spoiler located on the 35-percent-chord line of the lower wing surface inboard of the vertical tail are shown in figure 5. All models used in the comparison incorporated duct inlets.

TESTS AND RESULTS

Test Conditions

The variation of test Reynolds number with Mach number for average test conditions is presented in figure 6. The degree of turbulence of the tunnel is not known but is believed to be small because of the high contraction ratio of the tunnel (15.7:1). The size of the model used in

the present investigation leads to an estimated choking Mach number of 0.95 based on one-dimensional-flow theory. However, inasmuch as no evidence of any choking phenomena was apparent even at a tunnel Mach number of 0.95, the semispan data are presented for the highest Mach numbers obtained for the sake of comparison with the wing-flow data.

The greater part of the semispan wind-tunnel tests were made for the complete model configuration for several control deflections. A limited amount of data were obtained with the vertical fins off at zero control deflection.

The tests were made with the fuselage partially submerged in the wall boundary layer and with some leakage around the support strut. The tunnel-wall boundary-layer thickness was about 2.5 inches based on 95 percent of free-stream velocity. The leakage through a $\frac{1}{8}$-inch gap around the model support was minimized by using the fuselage as an end plate.

Corrections

Jet-boundary corrections to the lift and drag measurements were determined by the method of reference 2. All coefficients and Mach numbers were corrected for blocking by the model and its wake (reference 3). The Mach number blockage correction varied from 1.004 at $M = 0.6$ to 1.040 at $M = 0.95$. The sting pitching-moment data have been corrected for the additional tare correction given on page 10 of reference 1.

Presentation of Results

A table of the figures presenting the results is given below:

	Figure
I. Basic Semispan Model Data	
A. Longitudinal characteristics, fins on	7 to 8
B. Longitudinal characteristics, fins off	9
C. Effects of spoiler deflection, fins on	10
II. Comparison of Semispan, Sting, and Wing-Flow Data	
A. Variation of $\left(\partial C_L/\partial\alpha\right)_M$ with Mach number, fins on	11
B. Variation of $\left(\partial C_L/\partial\alpha\right)_M$ with Mach number, fins off	12
C. Variation of $\alpha_{C_L=0}$ with Mach number, fins on	13
D. Variation of $\alpha_{C_L=0}$ with Mach number, fins off	14
E. Variation of C_D with Mach number, fins on	15

DISCUSSION

Basic Semispan Wind-Tunnel Data

Basic aerodynamic characteristics.- It is noted that there is a small reduction in lift-curve slope in the low-lift range (figs. 7 and 8). This nonlinearity in the lift curves is attributed to tunnel-wall boundary-layer and strut-leakage effects which are discussed later in the portion of the paper dealing with the comparison of these data with those obtained by other methods. The data also indicate a reversal in control effectiveness for small control deflections at a Mach number of 0.96 (fig. 7(l)). The control reversal appears to occur outside a practical flight range and should not be serious.

Spoiler controls.- Lower surface spoilers (fig. 5) were investigated as an auxiliary control device to be used in the event of loss of control in the high Mach range. The data (fig. 10) show that the spoilers have a negligible effect on the lift characteristics while producing an appreciable nosing-up pitching-moment increment throughout the entire lift and Mach number range. The use of these spoilers as a means of dive recovery might be desirable in the high-speed range where the control effectiveness is greatly reduced. At a Mach number of 0.94, for example, the spoiler effectiveness is equivalent to about 4° of negative control deflection.

No drag data are presented for the spoiler tests (fig. 10) because of difficulties encountered with the drag balance.

Comparison with Sting Data and Unpublished Wing-Flow Data

Lift characteristics.- It is seen from the variation of lift-curve slope (low-lift range) with Mach number that there is good agreement between the data of the semispan model and wing-flow model for both fins

on and off (figs. 11 and 12). However, the data obtained with the sting-mounted model indicate substantially larger lift-curve slopes over most of the Mach number range particularly with fins on. The results of an unpublished investigation using the complete semispan model of the tailless airplane has shown that tunnel-wall boundary-layer and strut-leakage effects can cause the differences noted between the lift-curve slopes of the sting and the semispan data. Although these tests were made with the complete model, similar results could be expected for the model without vertical fins. The similarity of trends for the fins-on and fins-off data is evident from figures 11 and 12. The boundary layer on the F-51 wing-flow test vehicle was much smaller relative to the size of the wing-flow model, but indications are that the effects of leakage around the base of the model were appreciable. The Reynolds number for the wing-flow model varied from about 1.0×10^6 at the lowest Mach numbers to 2.0×10^6 at the highest Mach numbers.

The angle of attack for zero lift as obtained by the three testing techniques is in fairly good agreement for the vertical fins-off condition (fig. 14). With the vertical fins on (fig. 13), $\alpha_{C_L=0}$ occurs at about 0.6° higher angle of attack for the semispan model than for the sting model over most of the Mach number range. At the highest Mach numbers, however, $\alpha_{C_L=0}$ decreases to values more comparable to the sting data. The wing-flow data agree fairly well with the sting data at the lower Mach numbers but $\alpha_{C_L=0}$ is about 0.5° higher than the sting value at $M = 0.90$.

Drag characteristics.- It is seen from figures 15 and 16 that although the drag coefficient $\left(\text{at constant } C_L\right)$ is generally somewhat higher for the semispan model, the drag rise occurs at essentially the same Mach number as for the sting model. No drag data were available on the wing-flow model.

Pitching moment at zero lift.- Up to a Mach number of 0.91 all three methods are in fair agreement regarding the variation with Mach number of the pitching-moment coefficient at zero lift for the complete model (fig. 19(a)). With fins removed (fig. 19(b)) the data for the sting and semispan model show excellent agreement. The results for the semispan model appeared to be especially influenced by flow changes over the portion of the wing between the fuselage and the fin. These flow changes were brought about by different interaction effects of the boundary layer, leakage, and flow induced by the fin itself. From a comparison of the angle of zero lift, the lift-curve slopes, and the pitching moment at zero lift, it appears that these various interaction effects on the semispan model were less severe for the fin-off configuration.

There are known to be some slight differences between the wing-flow model and the wind-tunnel model due to constructional inaccuracies, and these differences, together with the indeterminate leakage condition at the root of the wing-flow and semispan models, may be partially responsible for whatever differences are noted in the comparison of the data.

Stability and control.- The curve of $\left(\partial C_m/\partial C_L\right)_M$ at low C_L for the complete semispan model (fig. 17) indicates an almost constant aerodynamic center at about 23.5-percent mean aerodynamic chord up to $M = 0.85$. Between a Mach number of 0.85 and 0.96 there is a large stabilizing shift in the aerodynamic-center location of about 10-percent mean aerodynamic chord. The sting data indicate an aerodynamic-center location generally about 2.0-percent mean aerodynamic chord more rearward of the basic semispan data; whereas, the value of $\left(\partial C_m/\partial C_L\right)_M$ for the wing-flow model generally falls between the other two models. The large rearward aerodynamic-center shift is evident in the curves for all three models above a Mach number of 0.85. The agreement in $\left(\partial C_m/\partial C_L\right)_M$ between the various test methods is not quite as good for the vertical fin-off condition (fig. 18).

The control effectiveness $\left(\partial C_m/\partial \delta_a\right)$ at $C_L = 0$ and for small control deflections is in good agreement for the various test methods up to $M = 0.91$. At the highest Mach numbers a reversal in effectiveness is indicated from both the wing-flow and the larger scale semispan data. (See figs. 21 and 7(l).) The reversals in the semispan data however occur at higher lift coefficients than the wing-flow data and for elevator deflections outside the trim range.

The control deflection required for level flight at an altitude of 30,000 feet and a wing loading of 28 was computed from the data of the various models in order to evaluate the magnitude of trim change indicated at high subsonic speed (fig. 22). The variation of $\delta_{a_{trim}}$ with Mach number for the sting and semispan models was in good agreement, and forward stick movement was required to affect increases in speed up to $M = 0.87$. Above this Mach number a tucking-under tendency is manifested. Note that in the Mach number range between 0.95 and 0.975 the wing-flow model could be trimmed at several values of δ_a. This was caused by the reversal of control effectiveness at the high Mach numbers on the wing-flow model (fig. 21).

CONCLUSIONS

An investigation was made to determine the aerodynamic characteristics of a semispan model of a tailless airplane and to compare these results with available data on the tailless airplane from an investigation of a complete wind-tunnel model and a semispan wing-flow model. These data indicated the following conclusions:

1. The lift-curve slopes obtained for the semispan model and the wing-flow model were in good agreement, but both were generally lower than the value obtained for the sting model. The results of an unpublished investigation have shown that tunnel-wall boundary-layer and strut-leakage effects can cause the differences noted between the lift-curve slopes of the sting and the semispan data.

2. Fair agreement was obtained between the data of the three models as regards the variation of pitching-moment coefficient with lift coefficient for various elevator deflections. However, in the Mach number range between 0.94 and 0.97, control reversal was indicated in the wing-flow data near zero lift; whereas, these same trends were indicated in the larger scale semispan data at somewhat higher lift coefficients.

3. Good agreement was obtained for the semispan and sting models in regard to the drag rise Mach number. The absolute drag coefficients, however, were somewhat higher for the semispan model than for the sting model.

4. All three test methods indicated a stable variation of control deflection with Mach number up to a Mach number of about 0.87 at an altitude of 30,000 feet and for a wing loading of 28. At higher Mach numbers all three methods also indicated a tucking-under tendency of similar abruptness and magnitude.

5. Tests of a 10-percent-span spoiler located on the 35-percent-chord line of the lower wing surface inboard of the vertical tail on the semispan wind-tunnel model were found to be equivalent to about 4° of negative control deflection throughout the Mach number range and may be useful as an auxiliary control in the transonic range.

Langley Aeronautical Laboratory
National Advisory Committee for Aeronautics
Langley Air Force Base, Va.

REFERENCES

1. Donlan, Charles J., and Kuhn, Richard E.: Estimated Transonic Flying Qualities of a Tailless Airplane Based on a Model Investigation. NACA RM L9D08, 1949.

2. Gillis, Clarence L., Polhamus, Edward C., and Gray, Joseph L., Jr.: Charts for Determining Jet-Boundary Corrections for Complete Models in 7- by 10-Foot Closed Rectangular Wind Tunnels. NACA ARR L5G31, 1945.

3. Herriot, John G.: Blockage Corrections for Three-Dimensional-Flow Closed-Throat Wind Tunnels, with Consideration of the Effect of Compressibility. NACA RM A7B28, 1947.

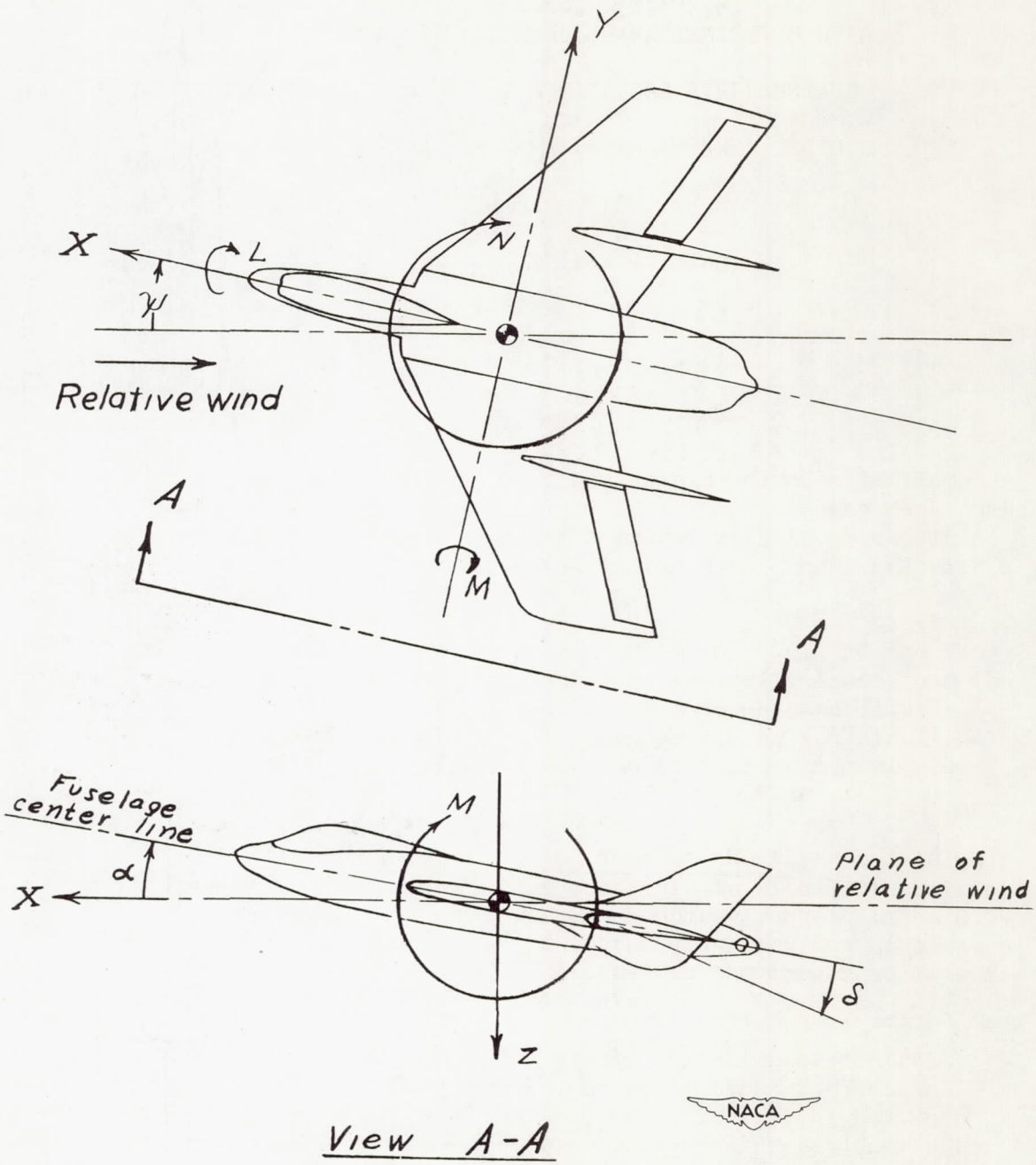

Figure 1.– System of axes and control–surface deflections. Positive values of forces, moments, and angles are indicated by arrows.

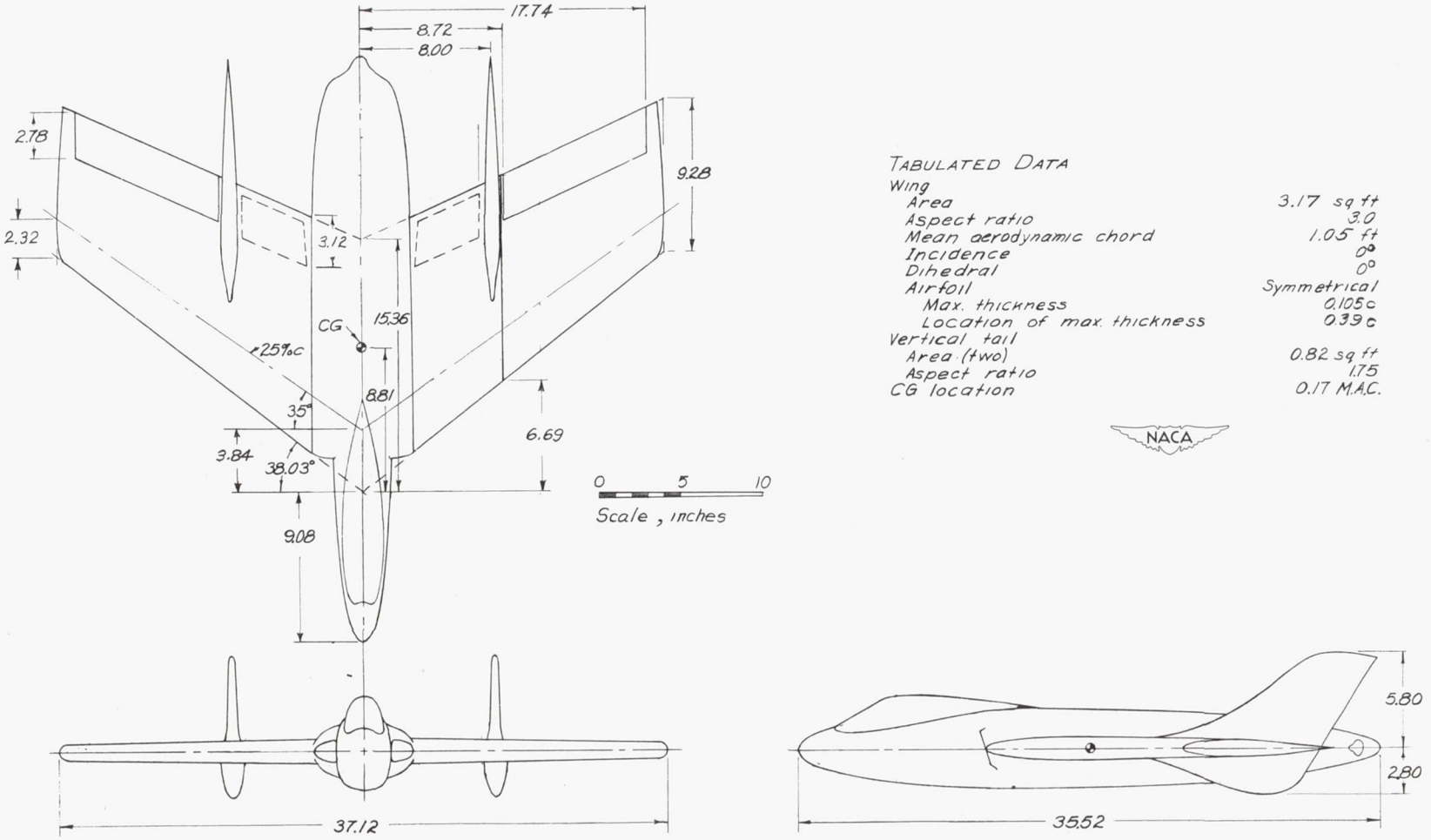

TABULATED DATA

Wing	
Area	3.17 sq ft
Aspect ratio	3.0
Mean aerodynamic chord	1.05 ft
Incidence	0°
Dihedral	0°
Airfoil	Symmetrical
Max. thickness	0.105 c
Location of max. thickness	0.39 c
Vertical tail	
Area (two)	0.82 sq ft
Aspect ratio	1.75
CG location	0.17 M.A.C.

NACA

Figure 2.- General arrangement of a model of a tailless airplane.

Figure 3.– The semispan model of a tailless airplane with vertical fin on, mounted on the Langley 7– by 10–foot high–speed tunnel ceiling.

Figure 4.– The semispan model of a tailless airplane with vertical fin removed, mounted on the Langley 7– by 10–foot high–speed tunnel ceiling.

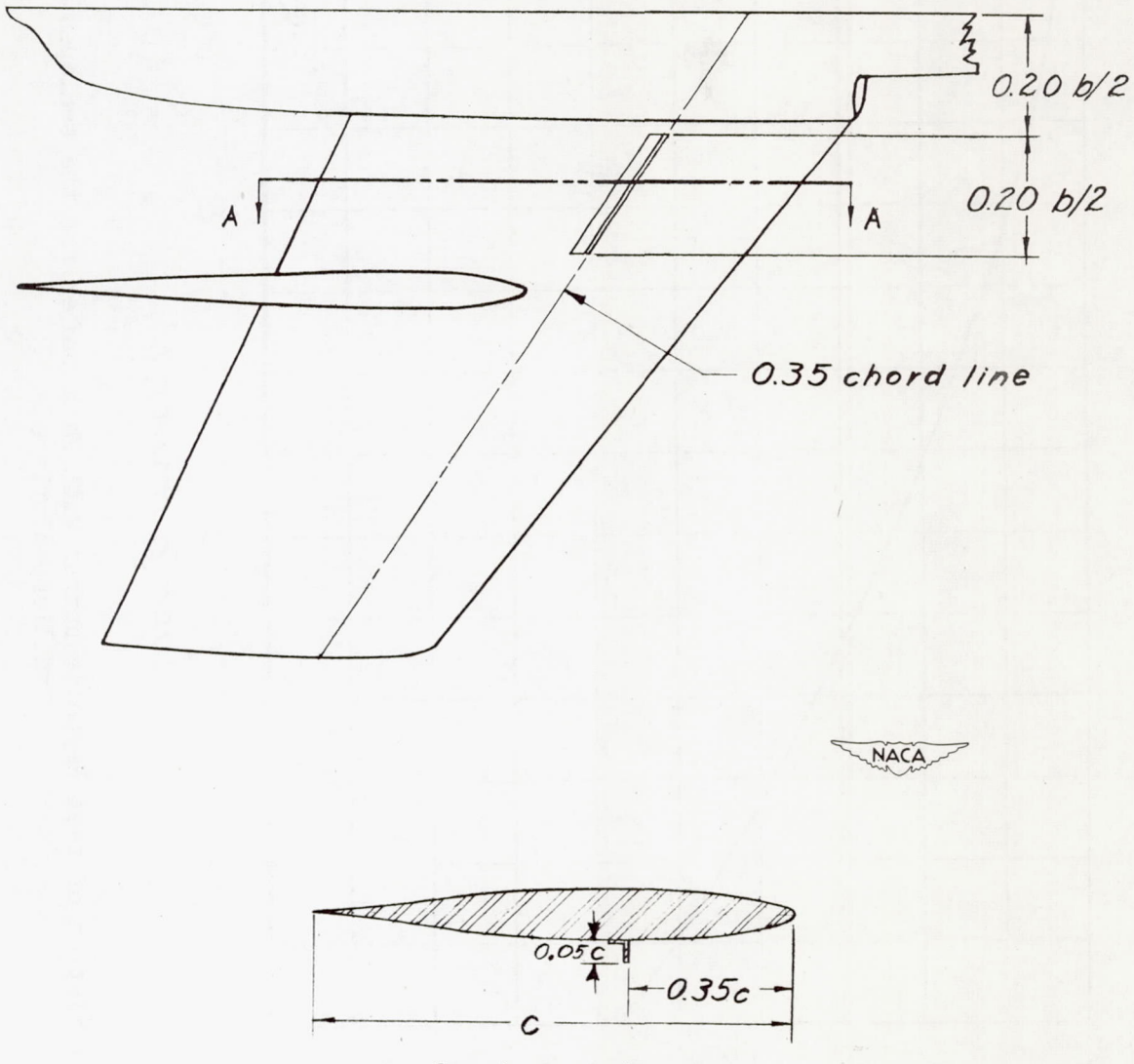

Figure 5.– Drawing showing location and size of spoiler on lower surface of the wing of the semispan model of a tailless airplane.

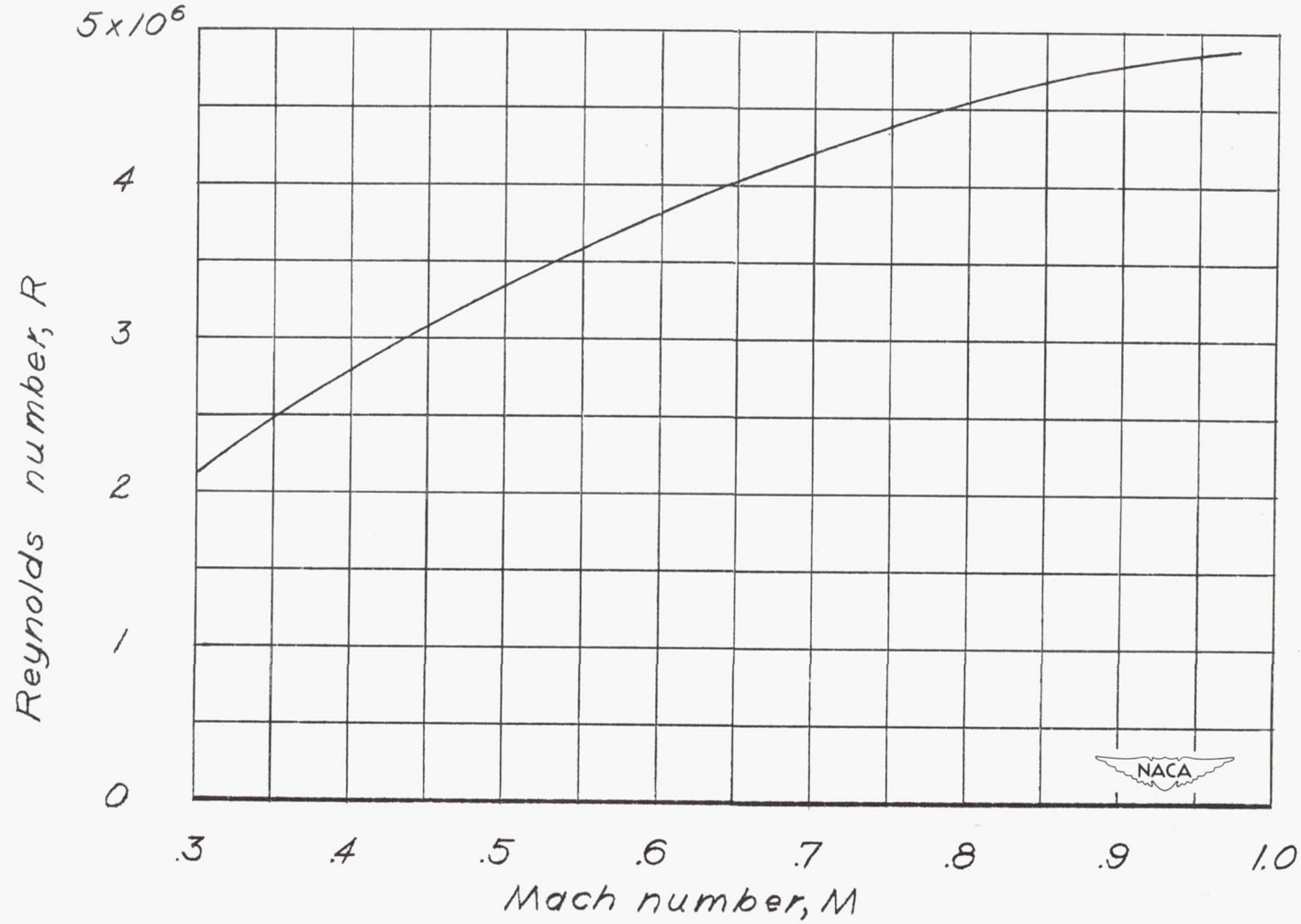

Figure 6.– Variation of test Reynolds number with Mach number for the semispan model of a tailless airplane.

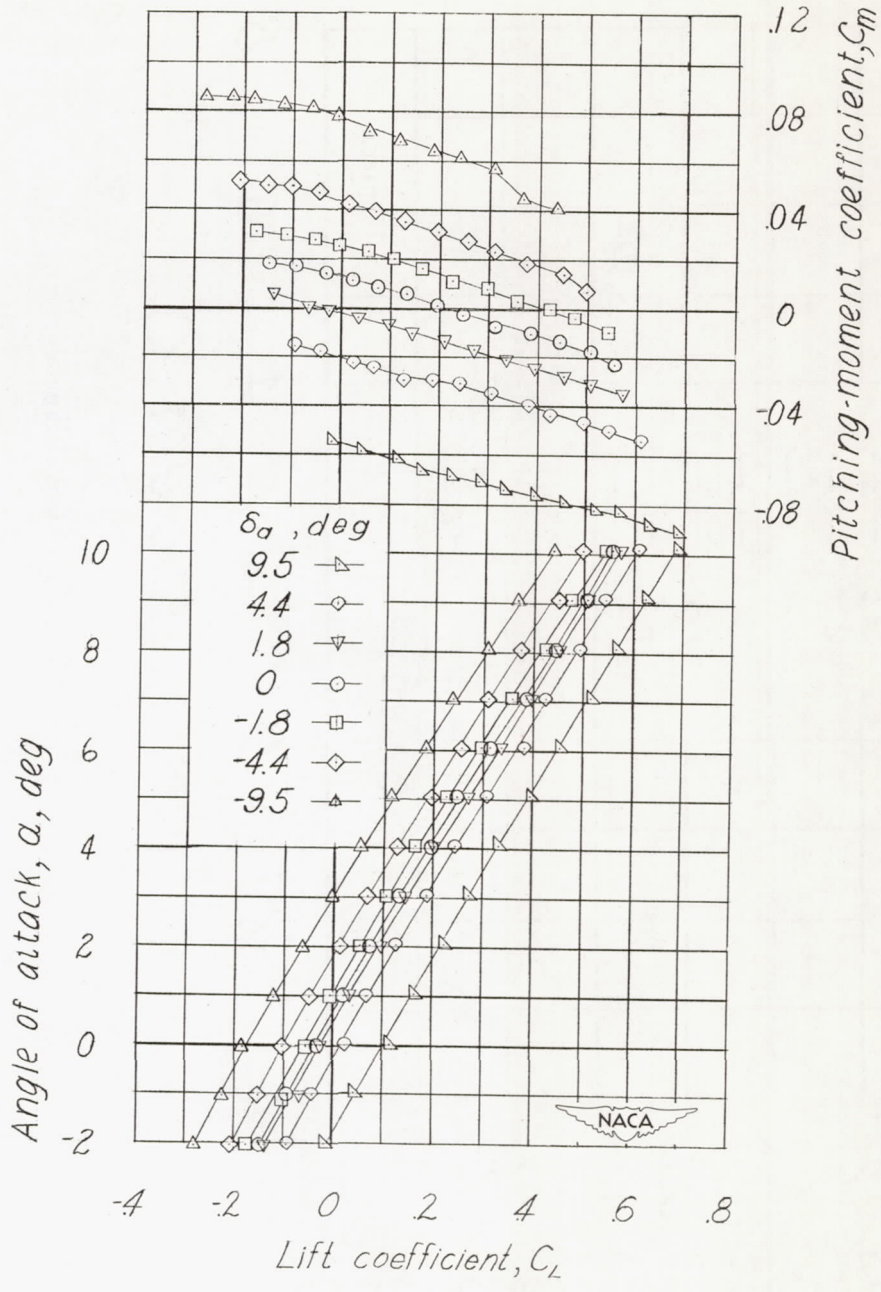

(a) M = 0.61.

Figure 7.– Effect of control deflection on the aerodynamic characteristics in pitch of the semispan model of a tailless airplane. Fins on.

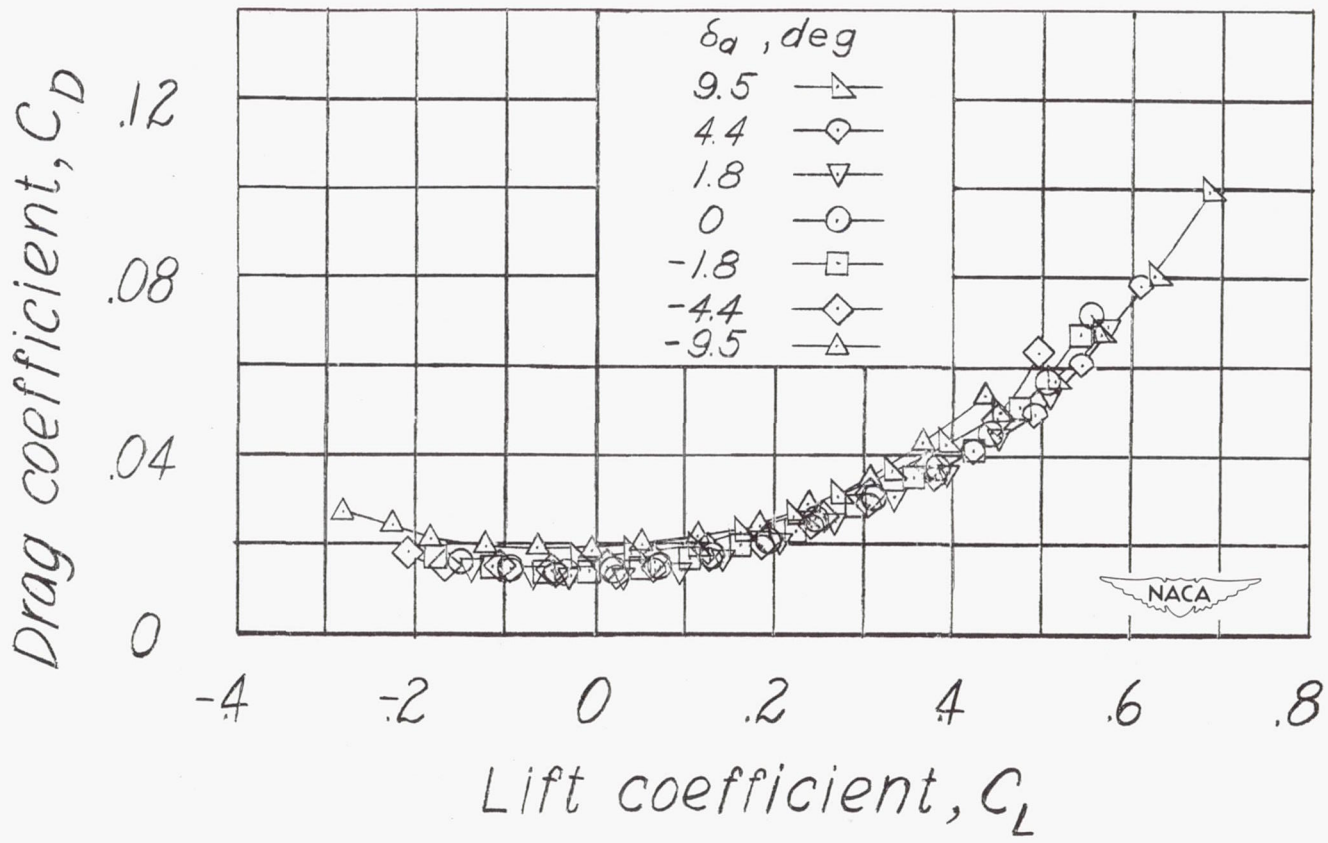

(a) M = 0.61. Concluded.

Figure 7.– Continued.

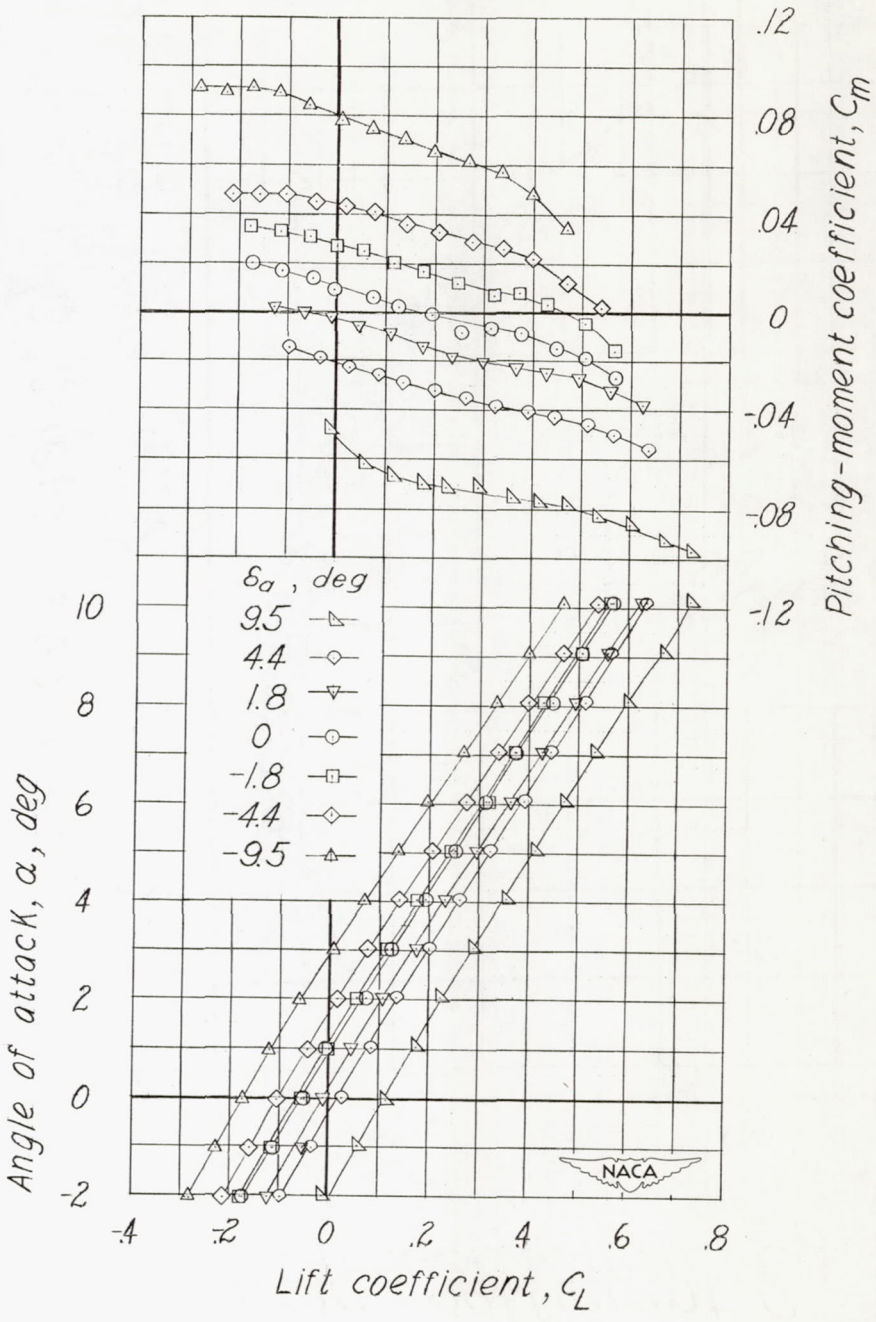

(b) M = 0.71.

Figure 7.– Continued.

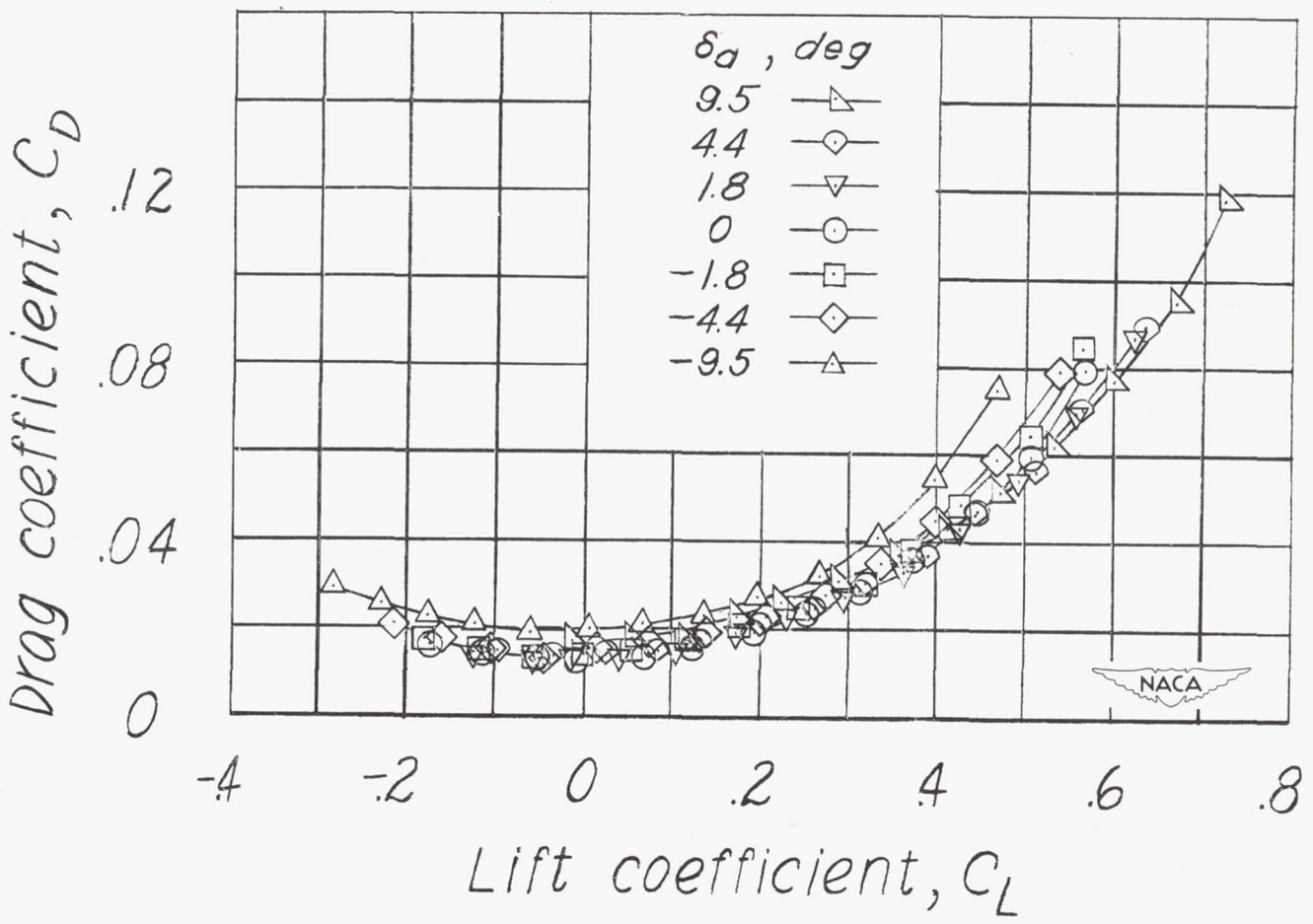

(b) M = 0.71. Concluded.

Figure 7.– Continued.

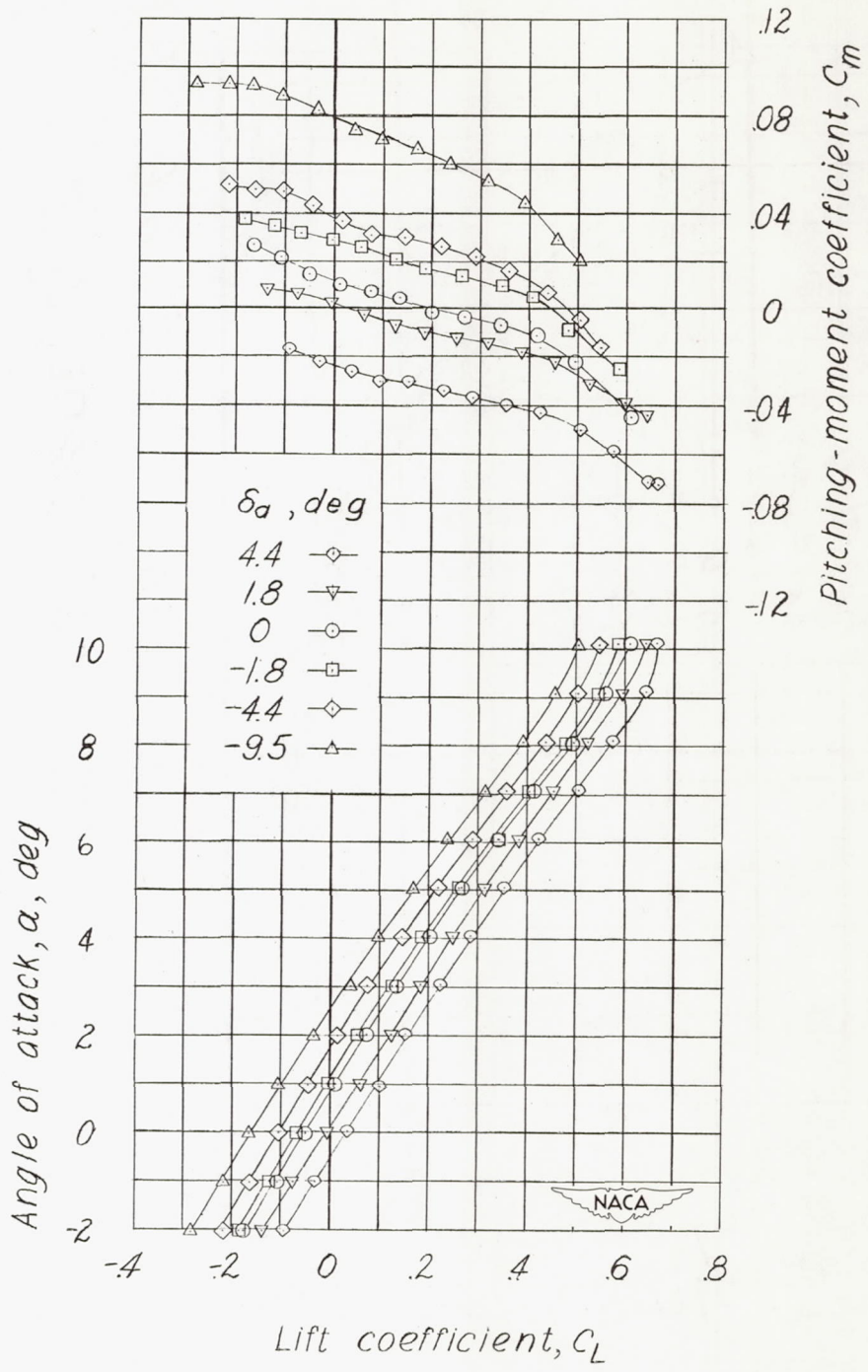

(c) M = 0.81.

Figure 7.– Continued.

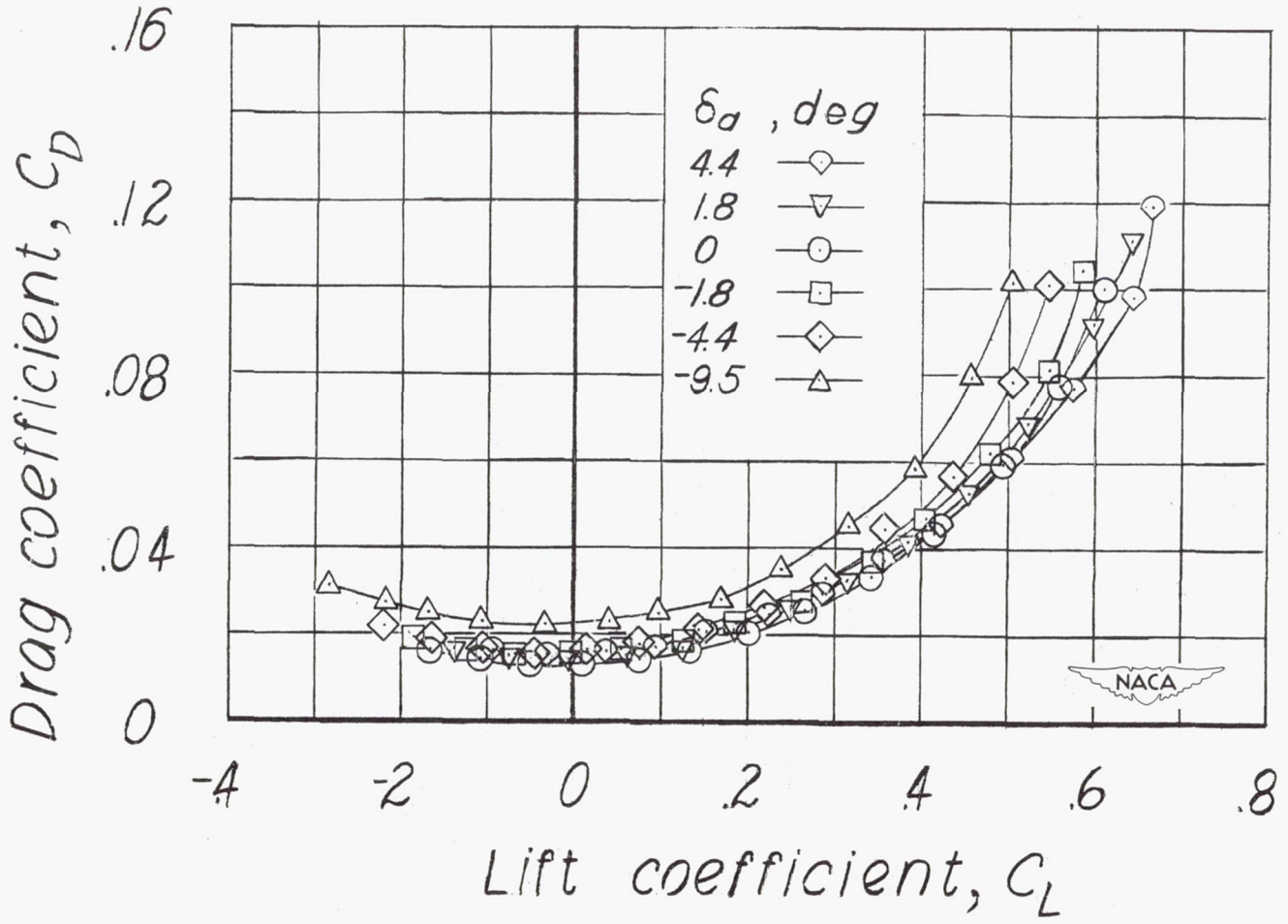

(c) M = 0.81. Concluded.

Figure 7.- Continued.

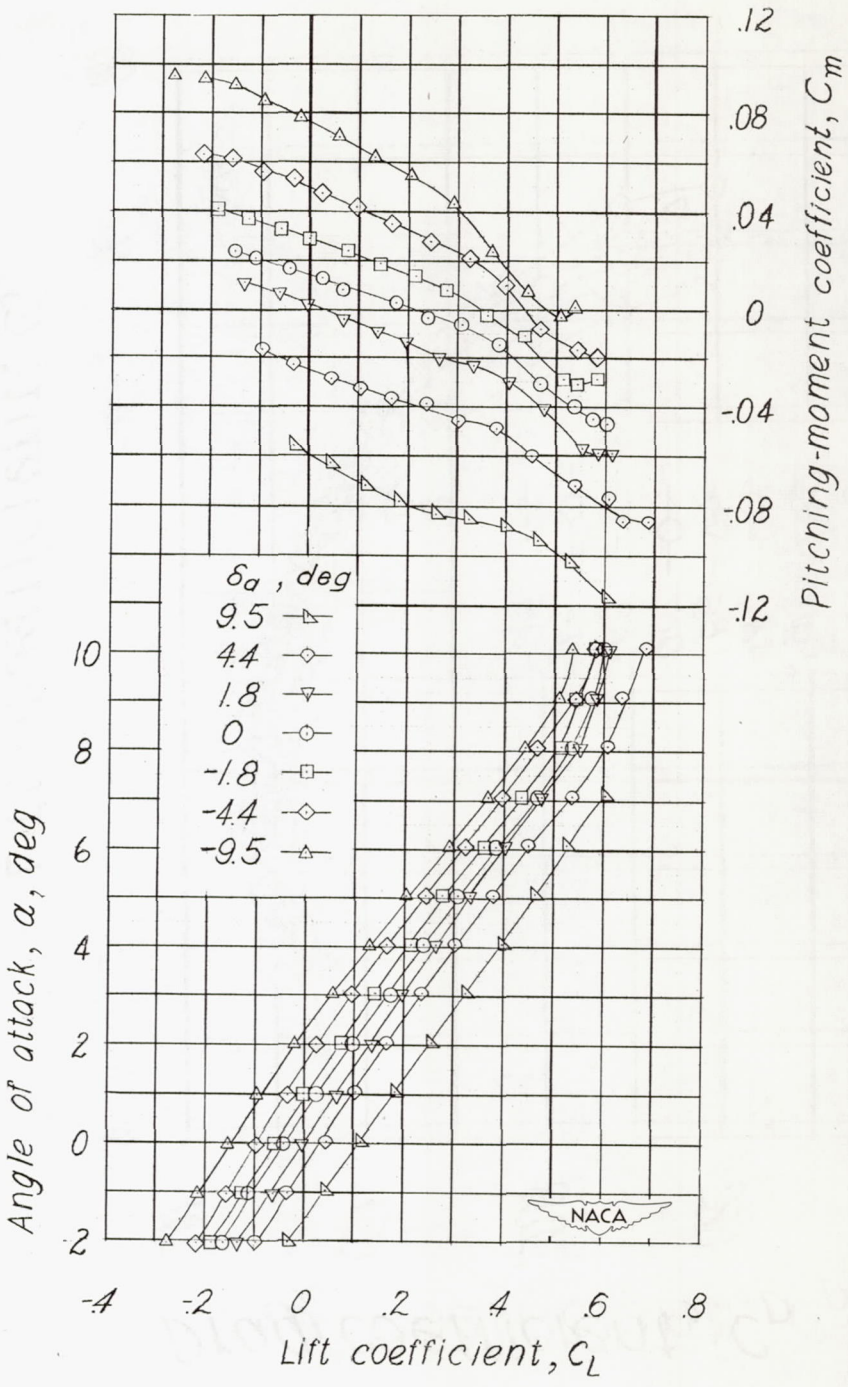

(d) M = 0.86.

Figure 7.– Continued.

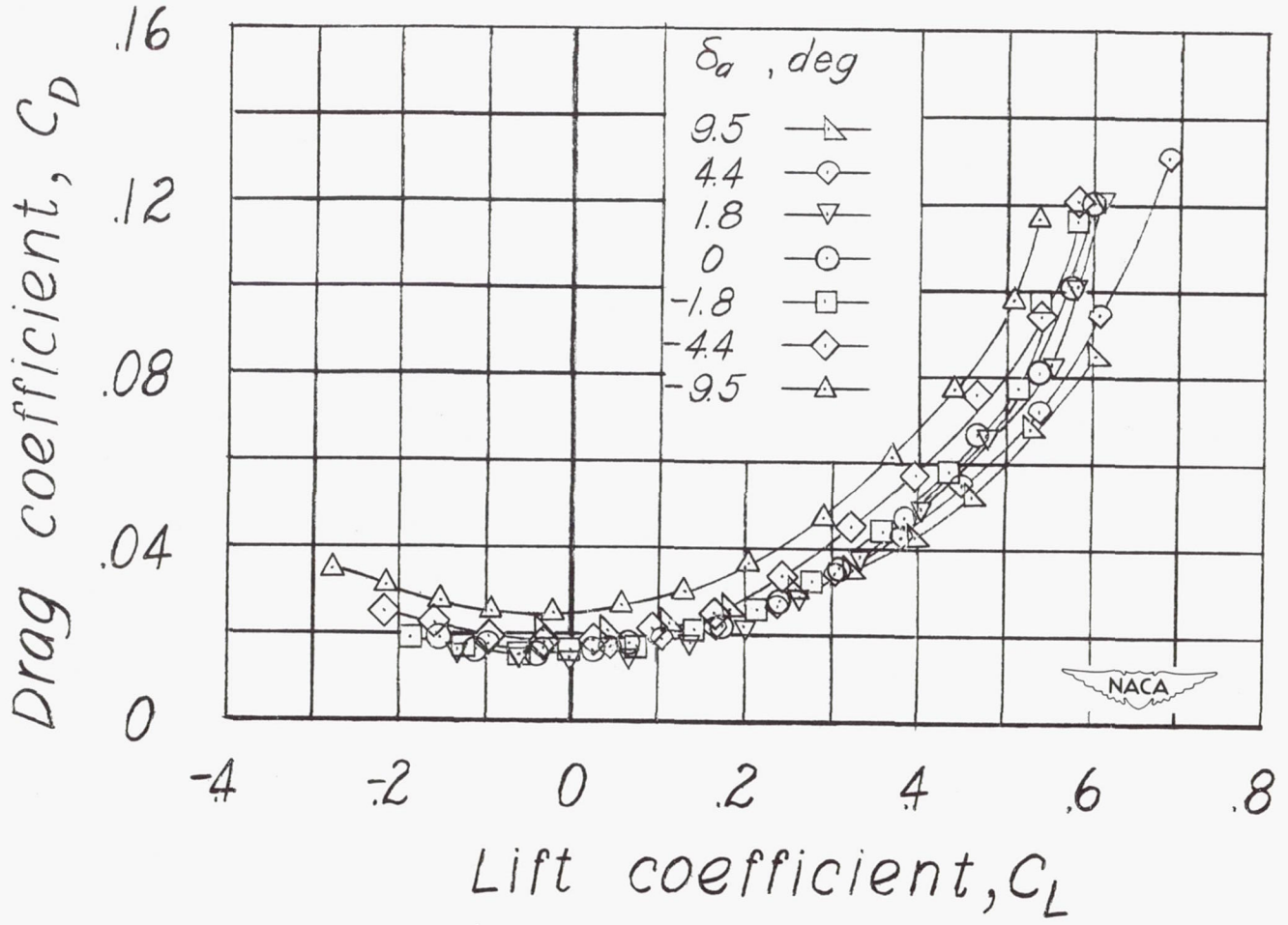

(d) M = 0.86. Concluded.

Figure 7.– Continued.

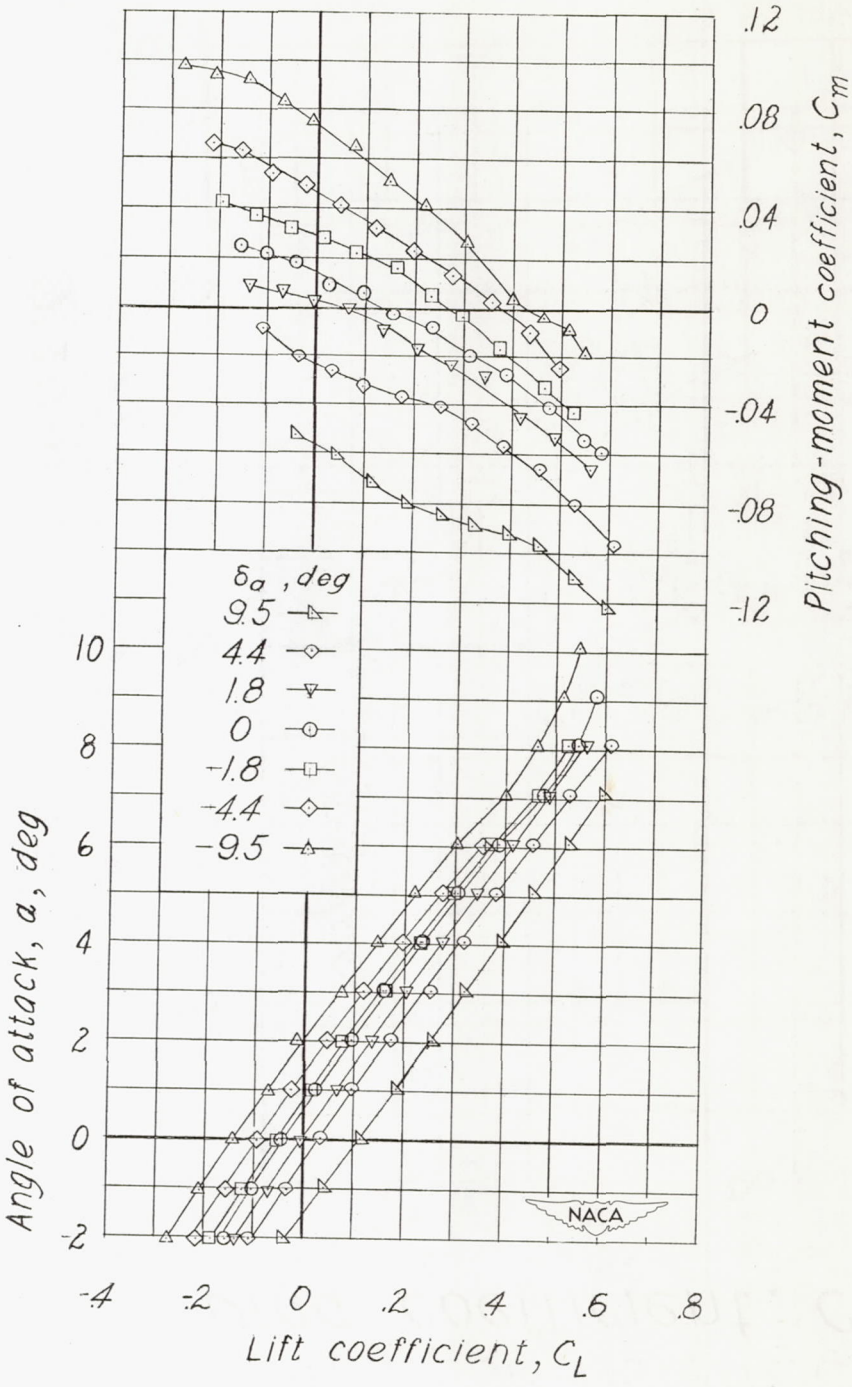

(e) M = 0.88.

Figure 7.– Continued.

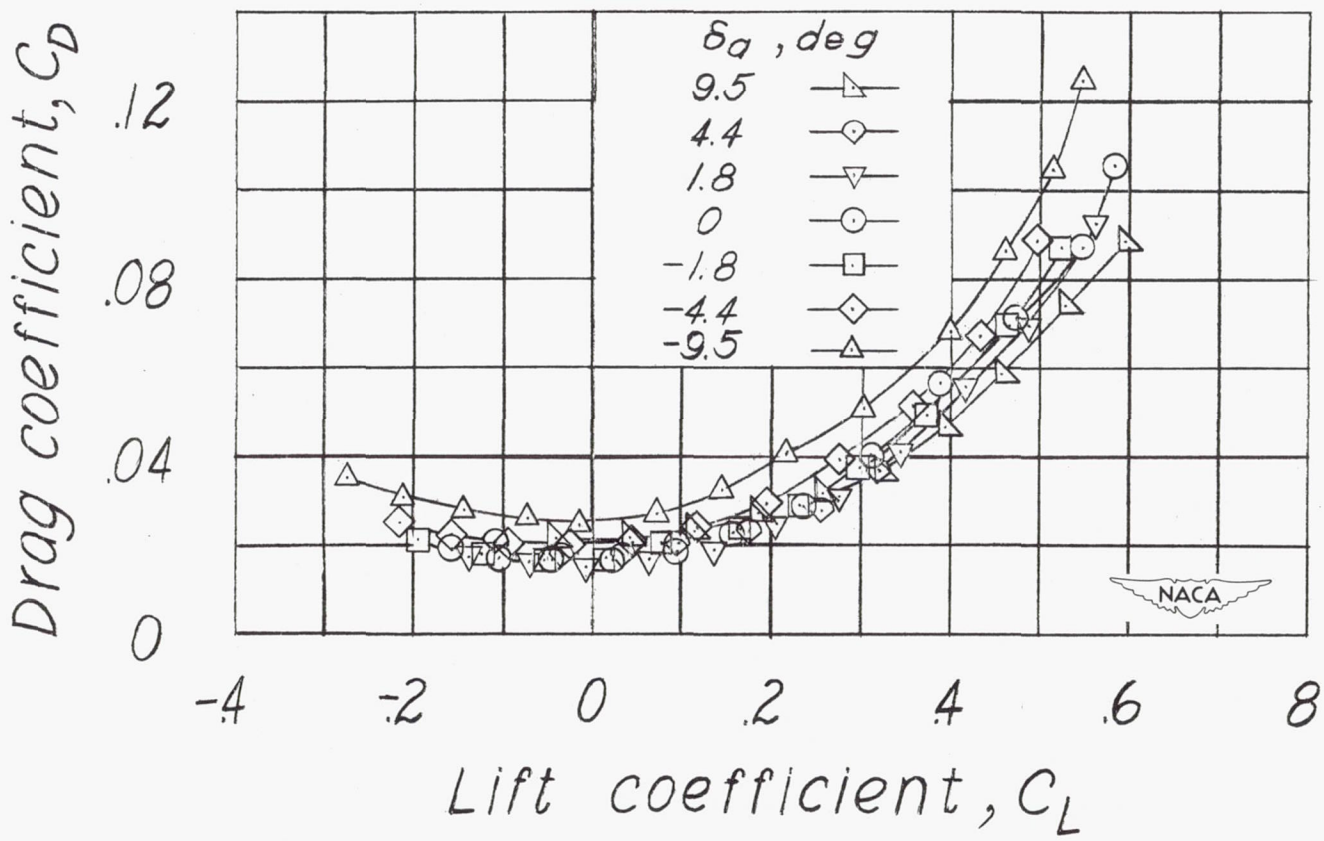

(e) M = 0.88. Concluded.

Figure 7.- Continued.

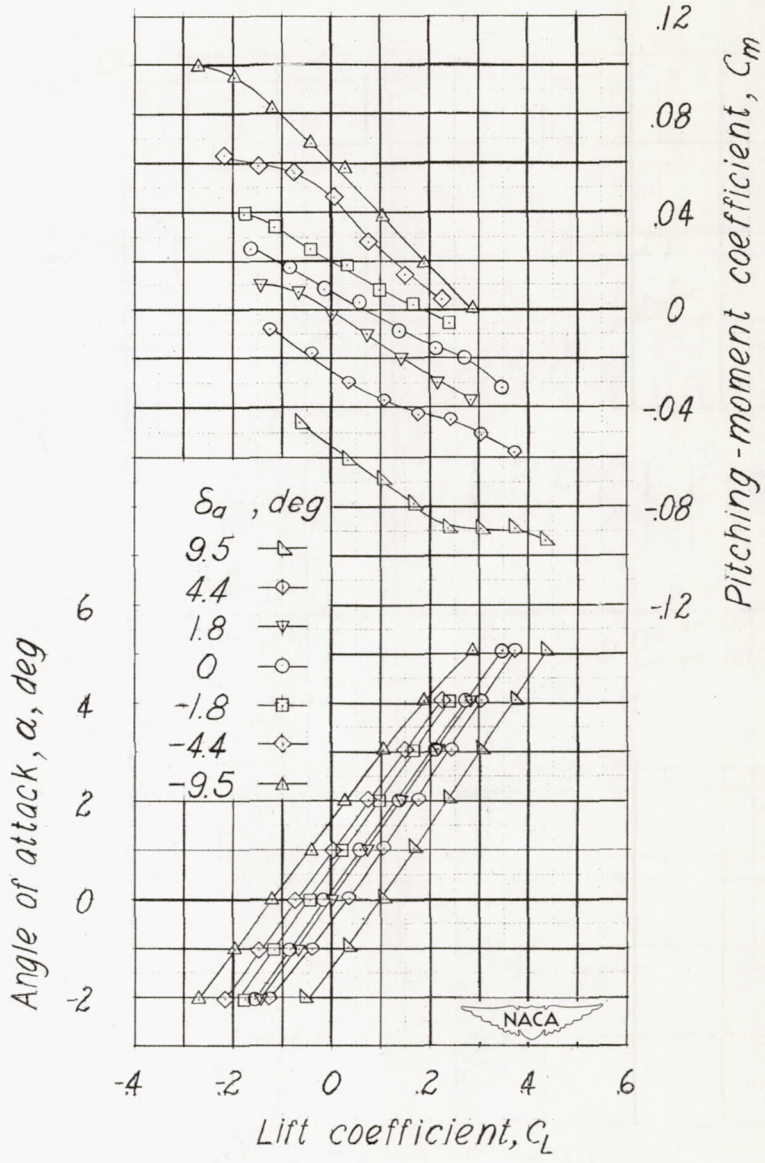

(f) M = 0.91.

Figure 7.– Continued.

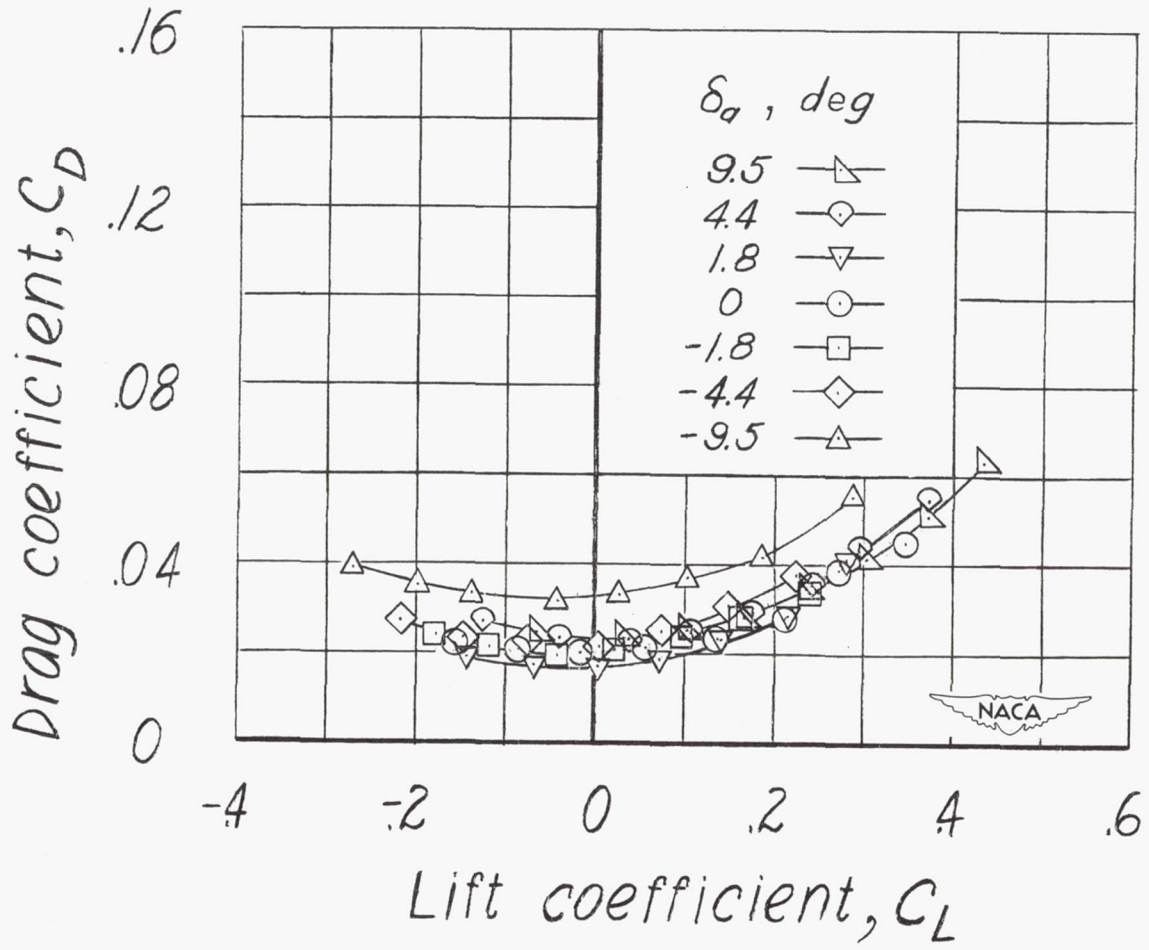

(f) M = 0.91. Concluded.

Figure 7.– Continued.

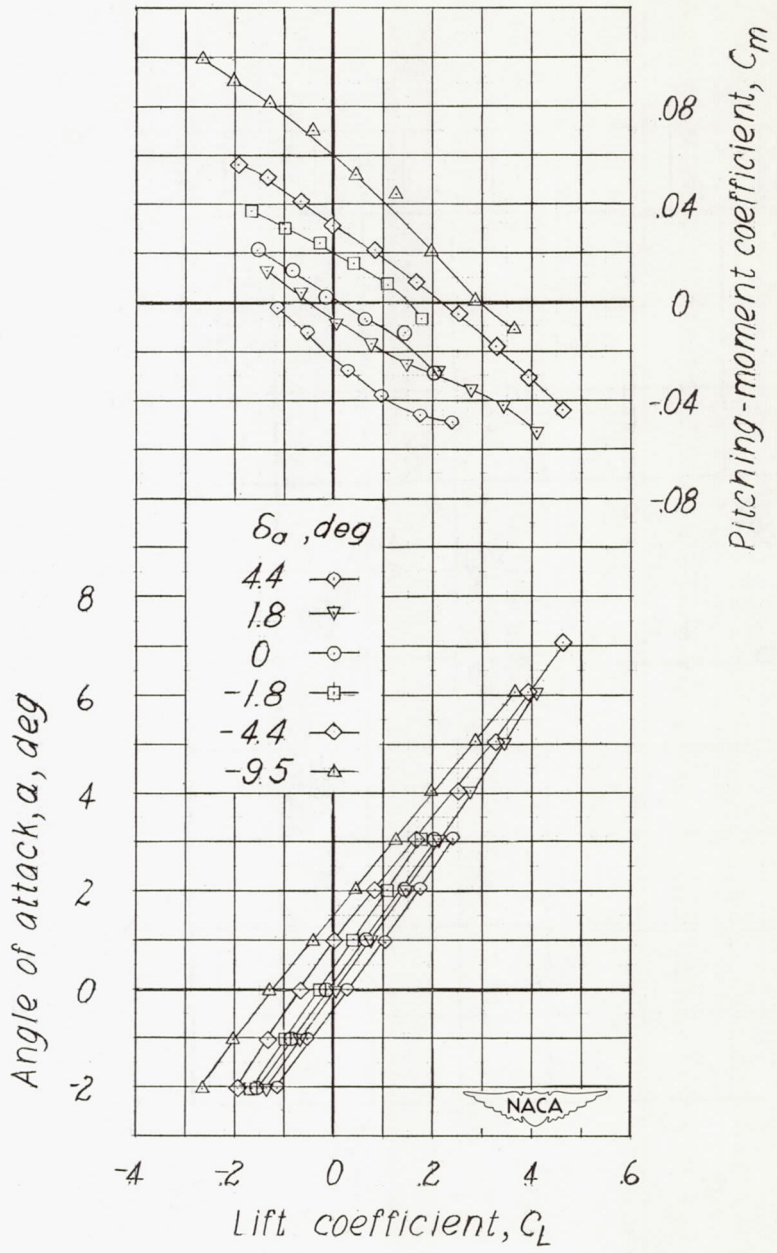

(g) M = 0.92.

Figure 7.– Continued.

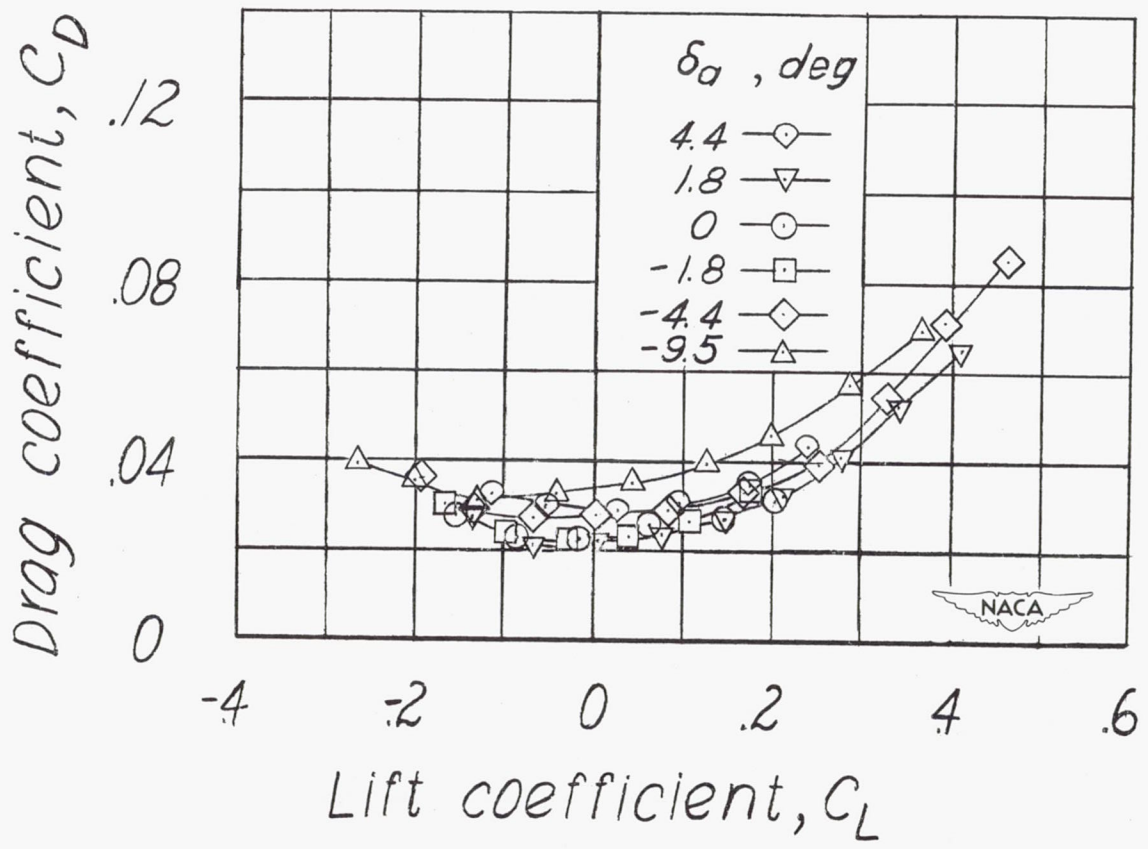

(g) M = 0.92. Concluded.

Figure 7.- Continued.

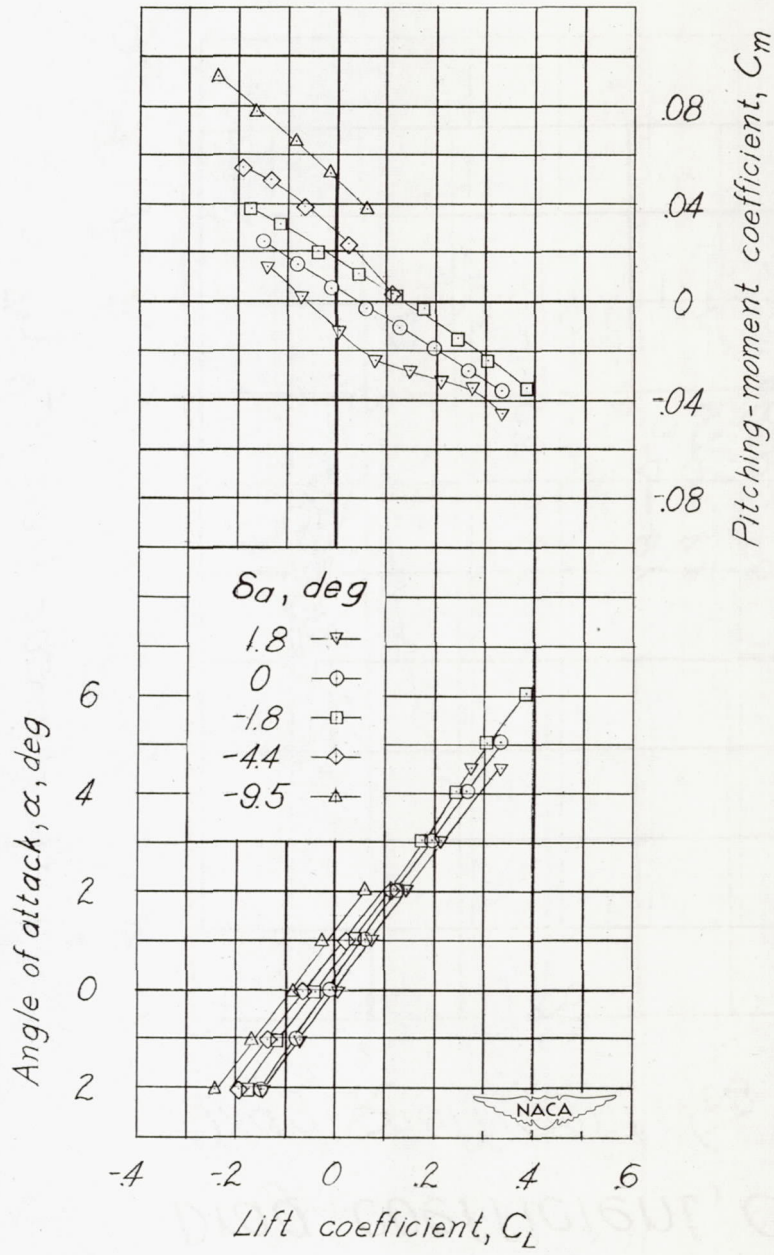

(h) M = 0.93.

Figure 7.– Continued.

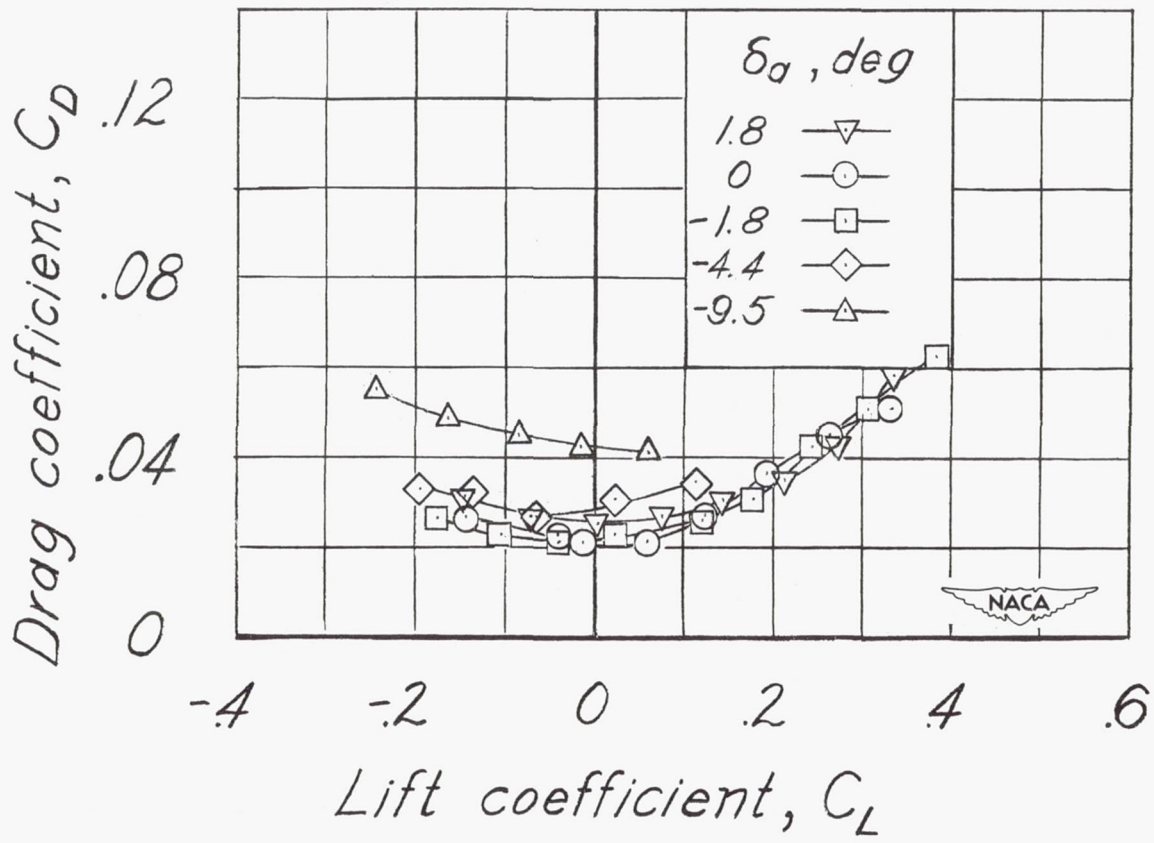

(h) M = 0.93. Concluded.

Figure 7.– Continued.

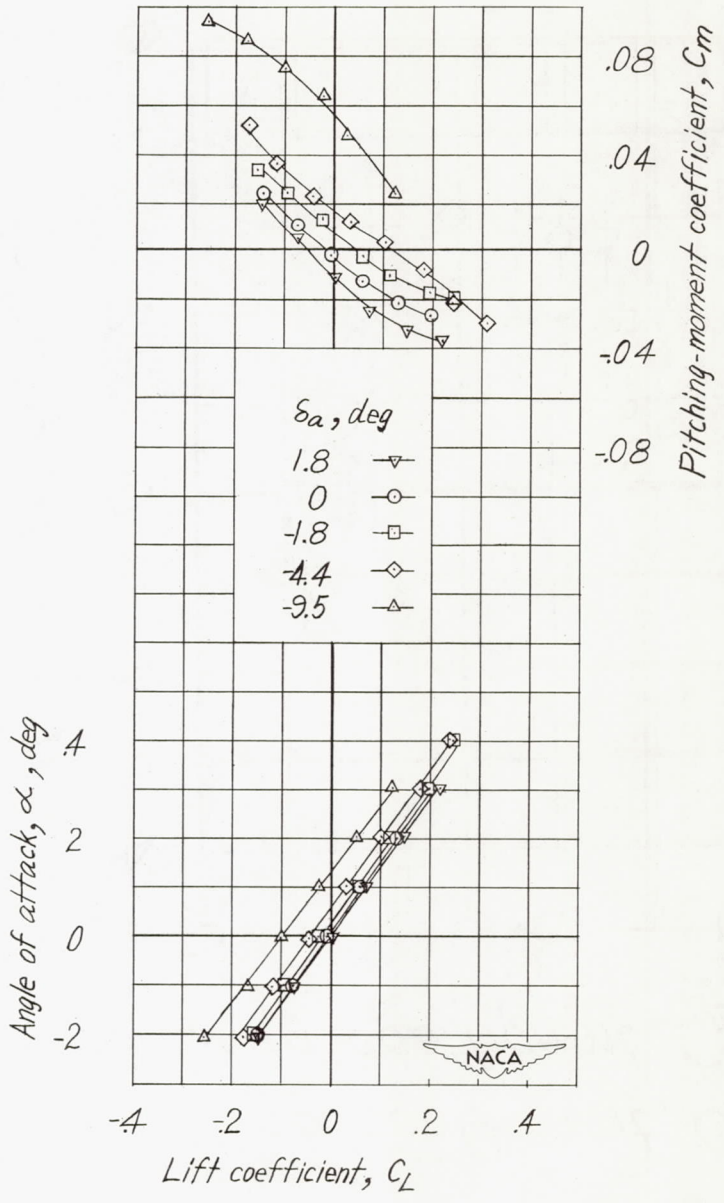

(i) M = 0.94.

Figure 7.– Continued.

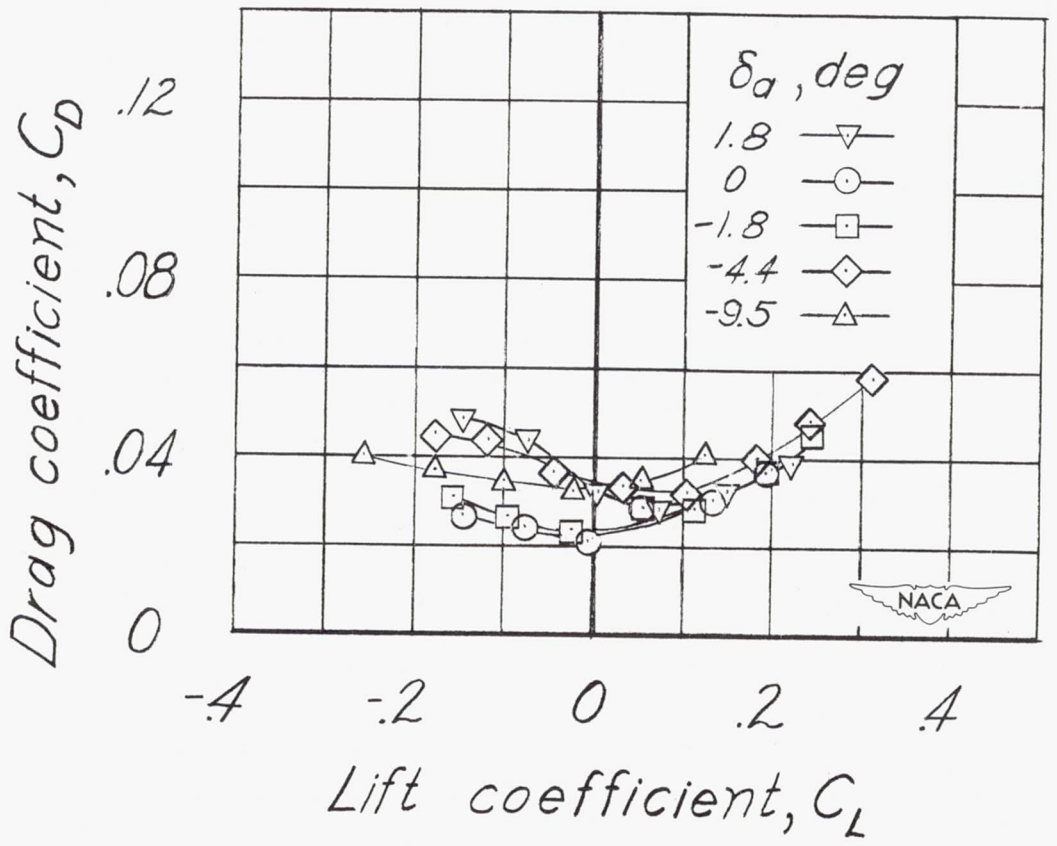

(i) M = 0.94. Concluded.

Figure 7.– Continued.

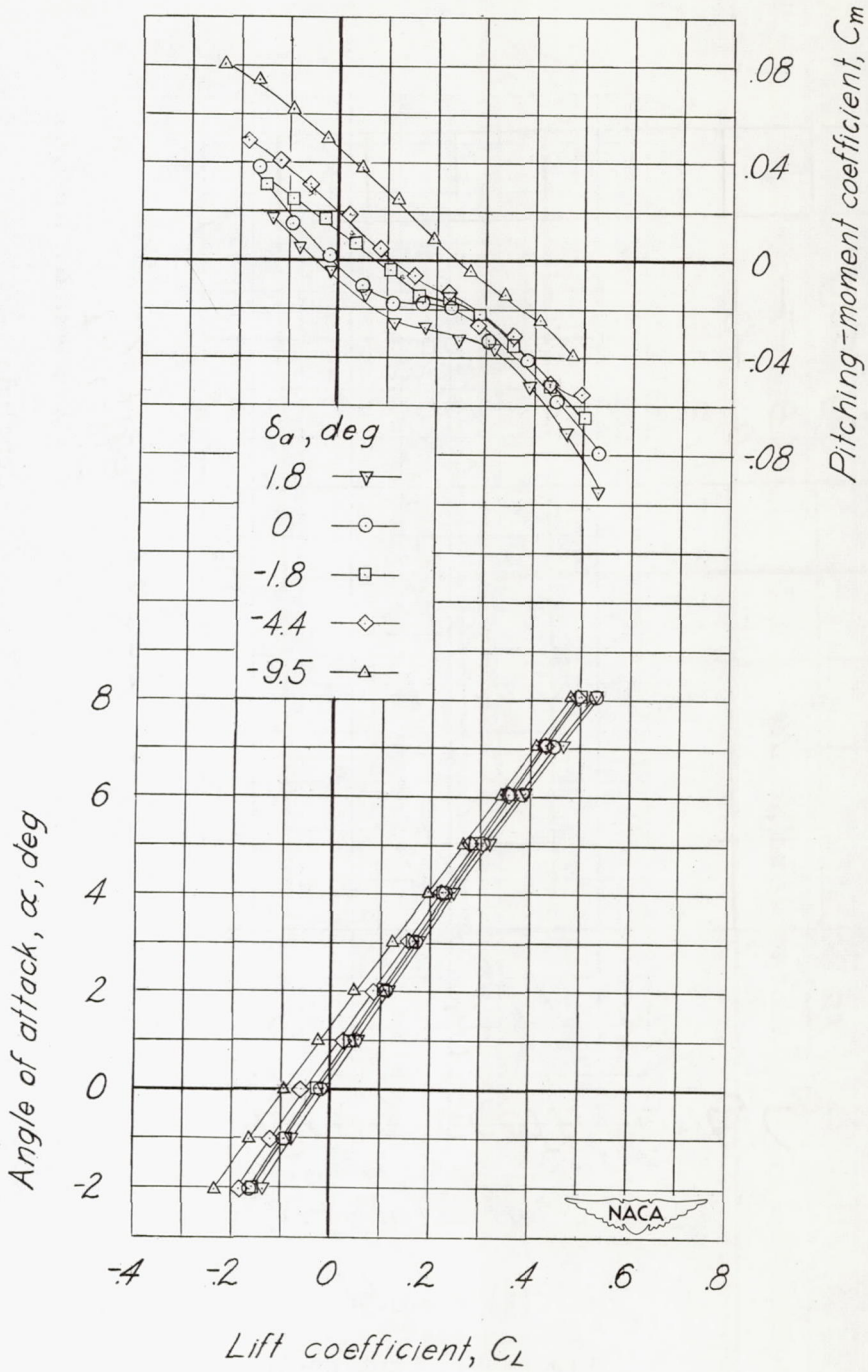

(j) M = 0.94 (check).

Figure 7.– Continued.

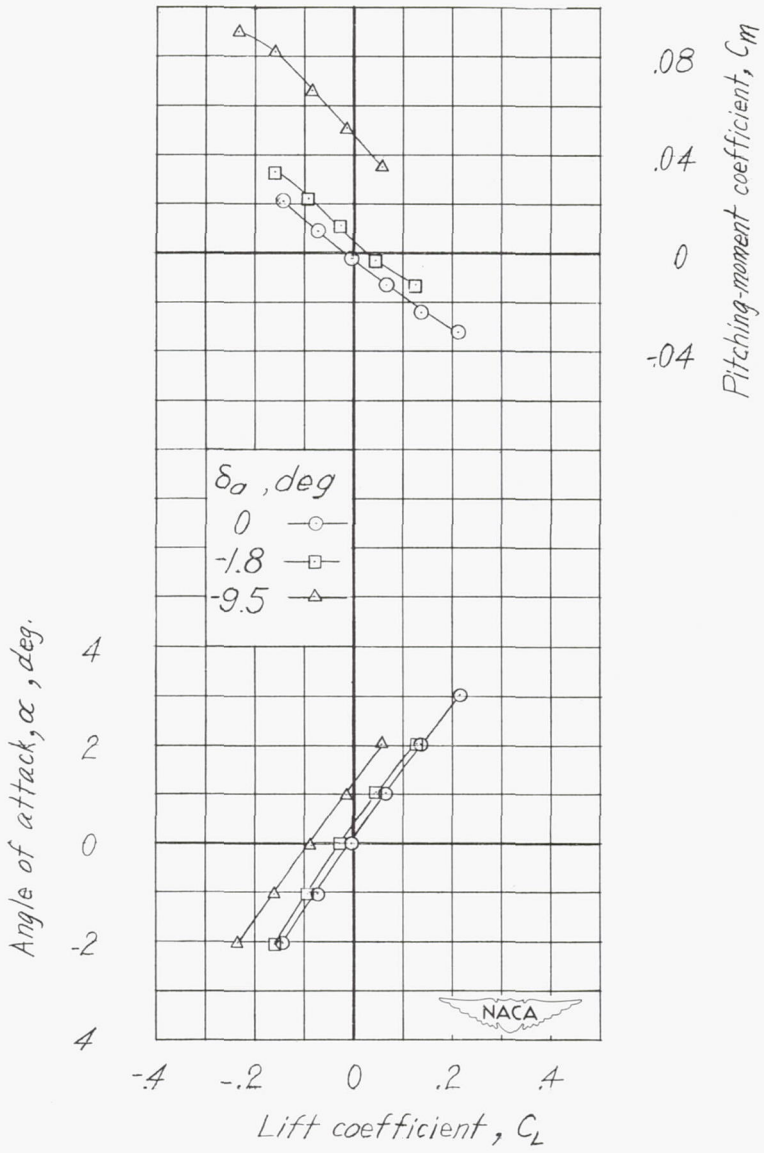

(k) M = 0.96.

Figure 7.– Continued.

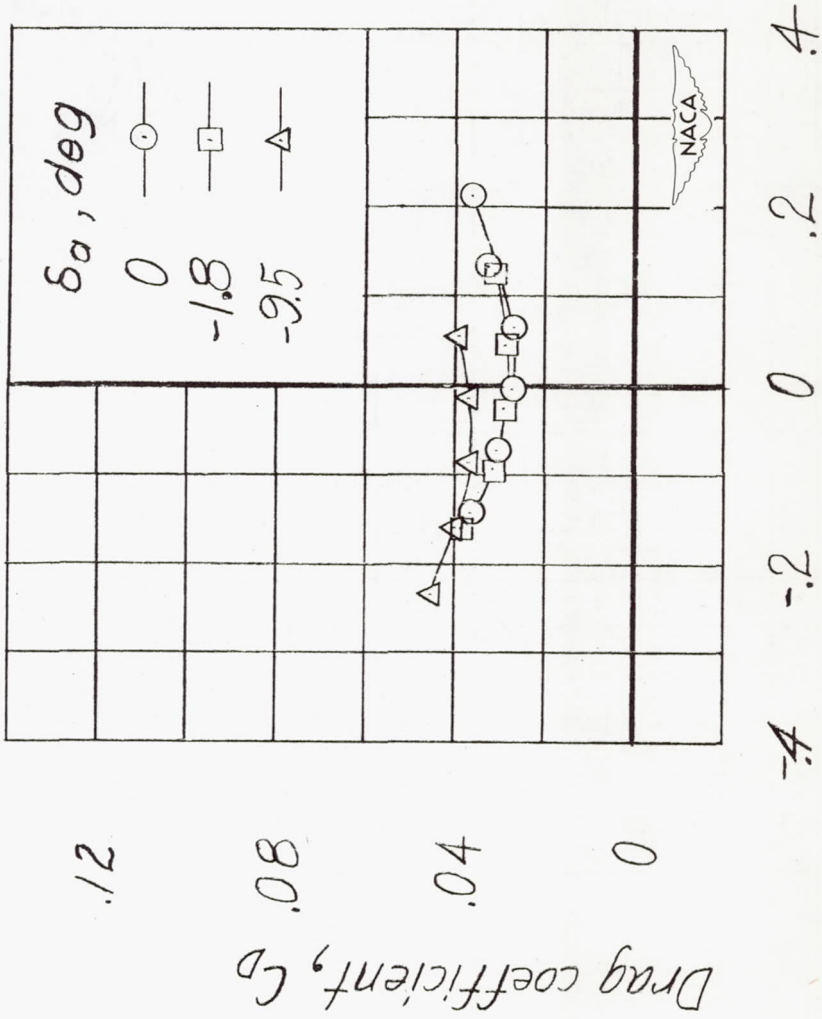

(k) M = 0.96. Concluded.

Figure 7.- Continued.

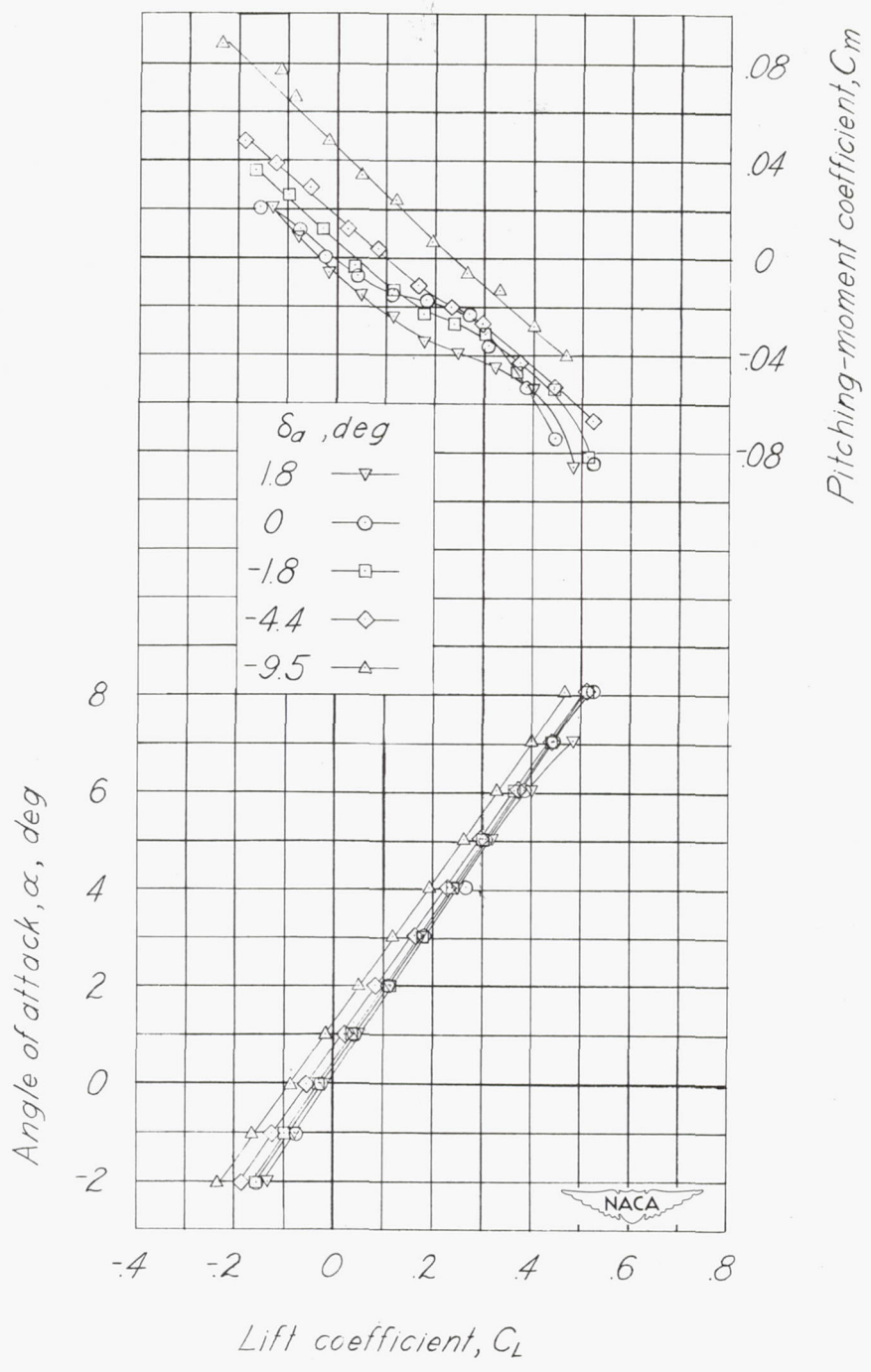

(l) M = 0.96 (check).

Figure 7.– Continued.

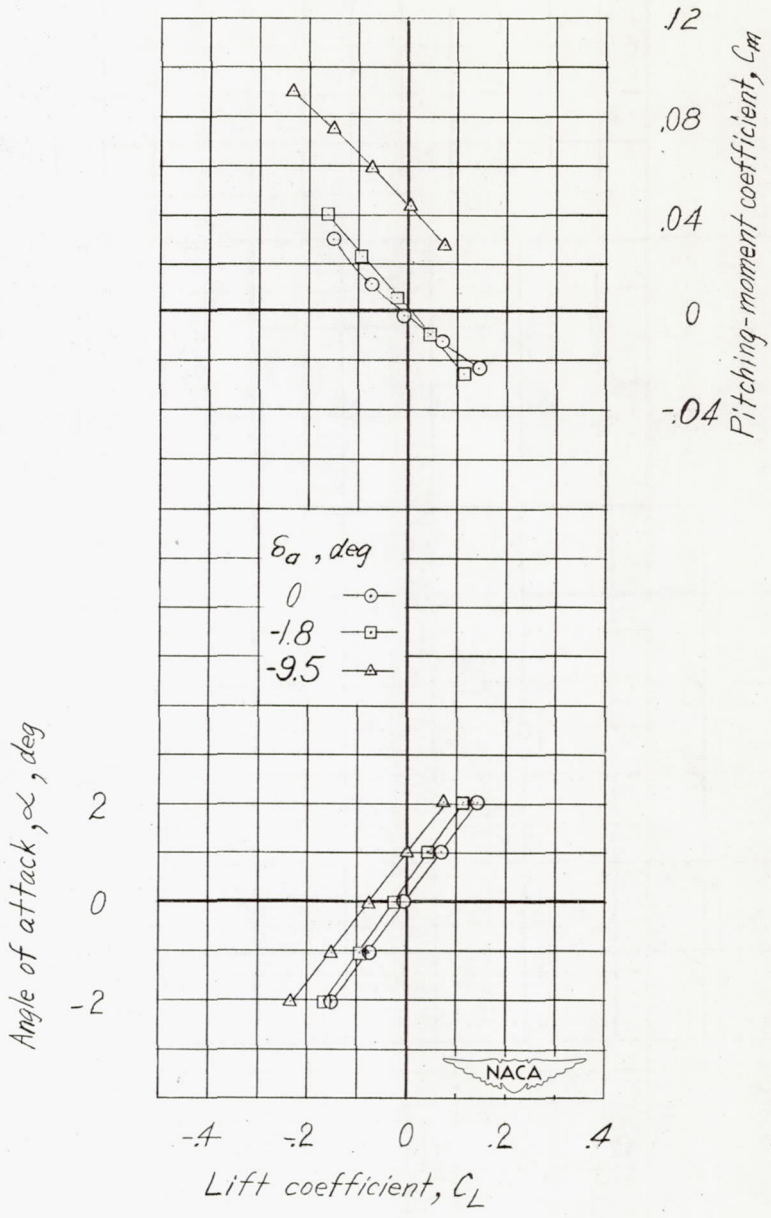

(m) M = 0.97.

Figure 7.– Continued.

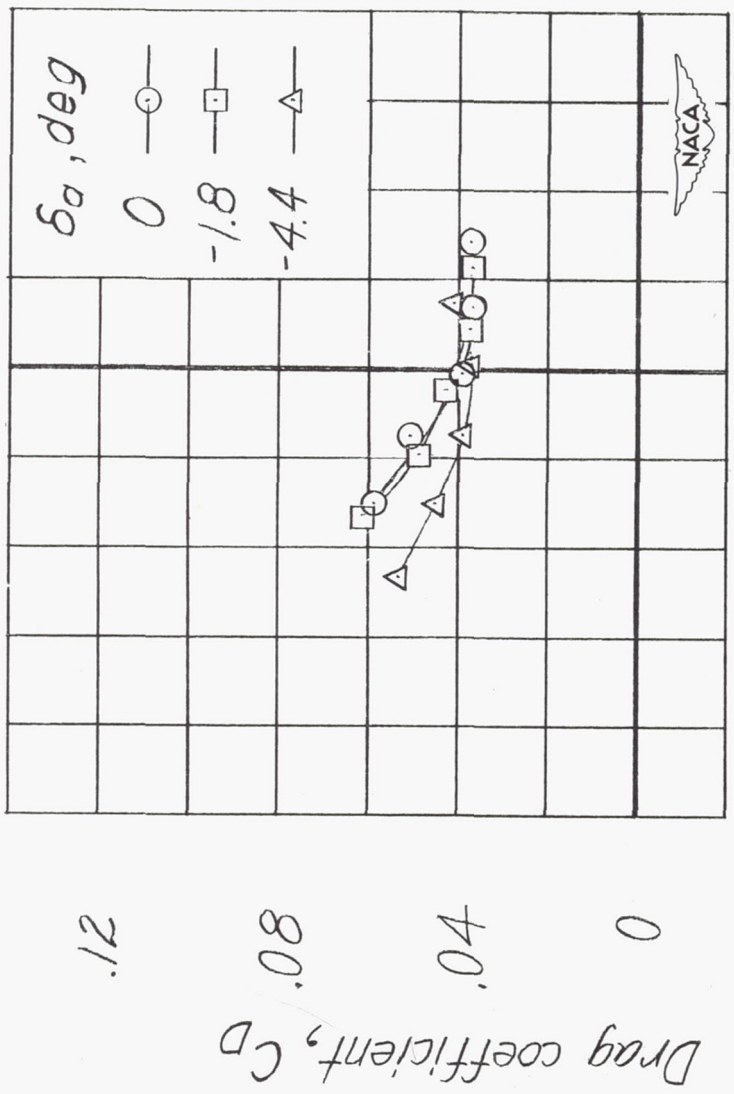

(m) M = 0.97. Concluded.

Figure 7.- Continued.

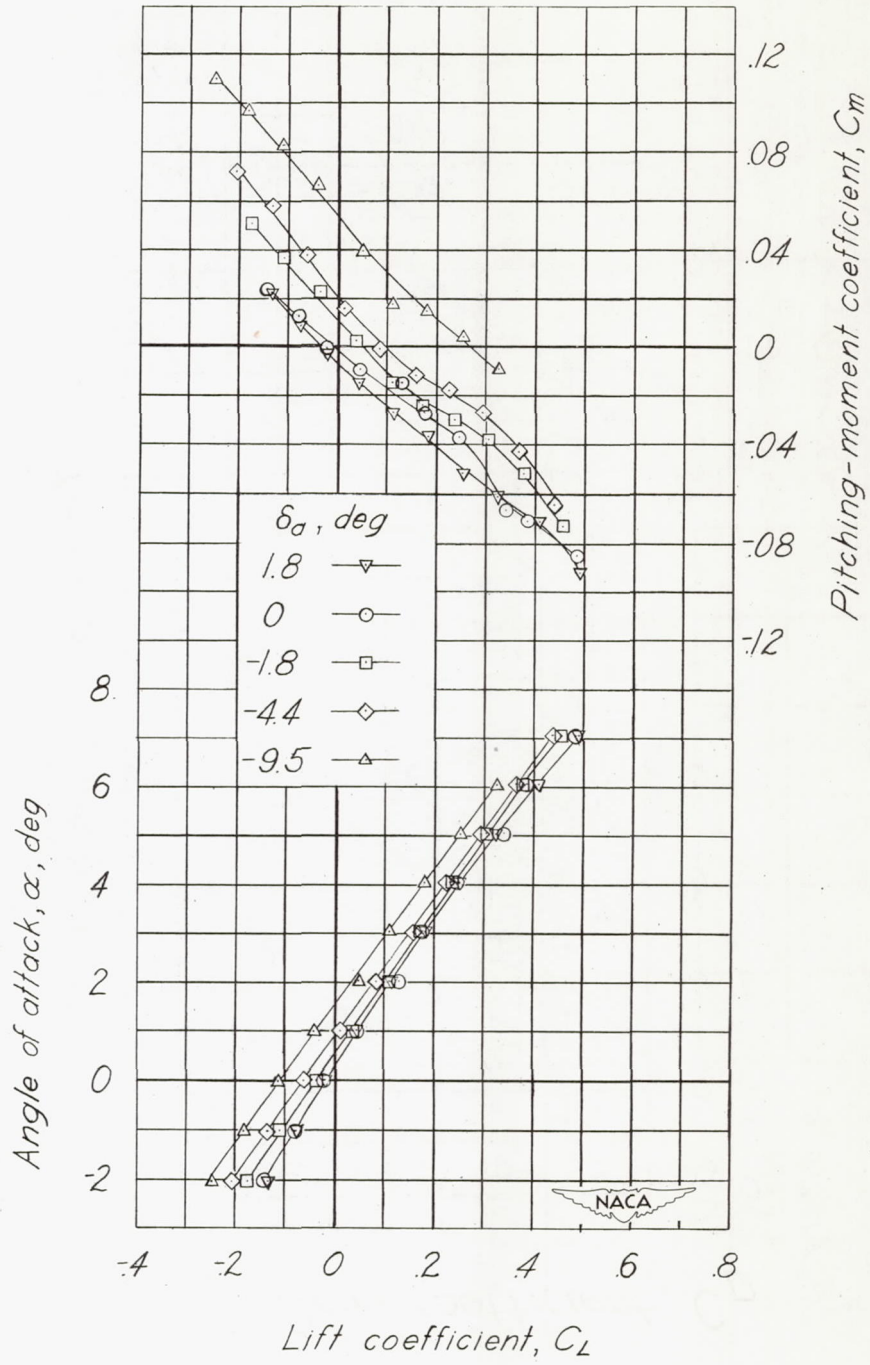

(n) M = 0.97 (check).

Figure 7.– Concluded.

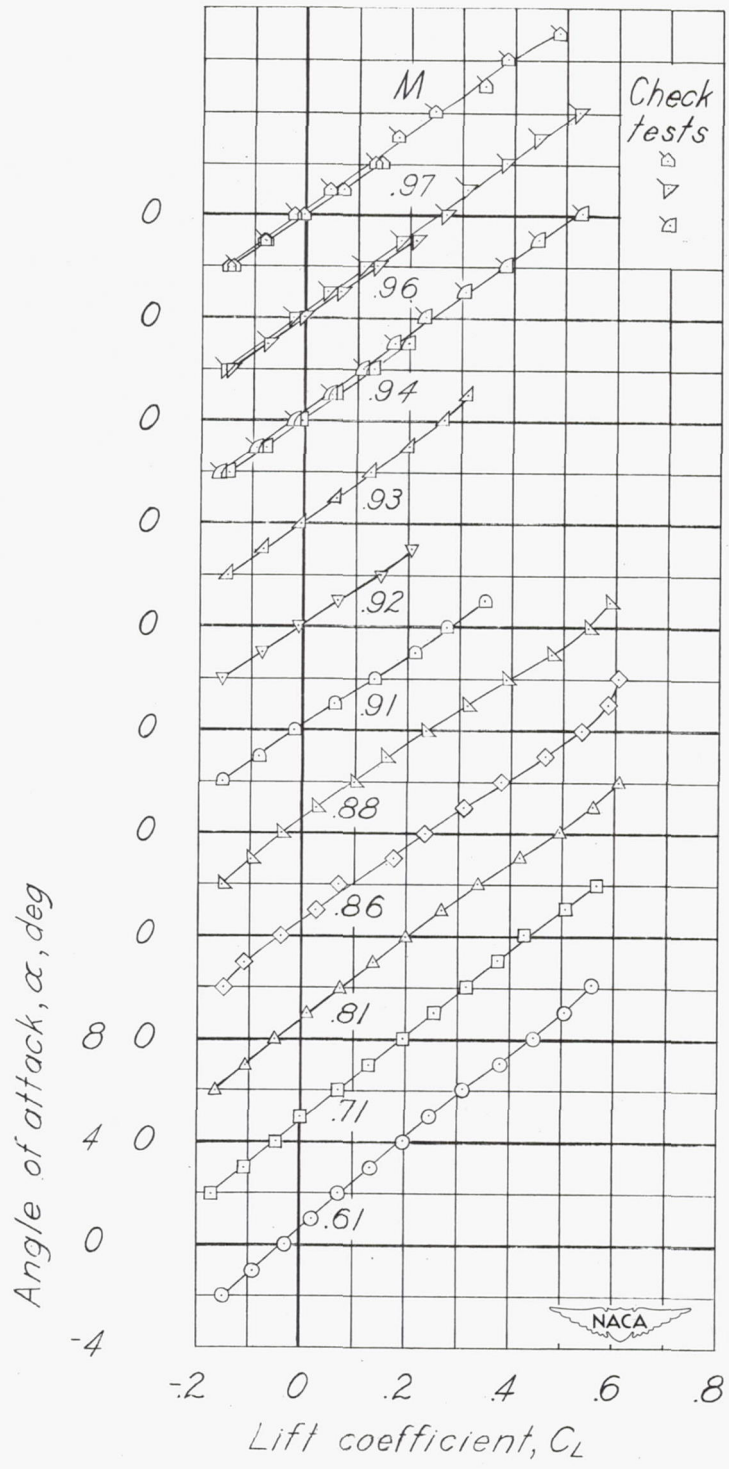

Figure 8.– Aerodynamic characteristics in pitch for various Mach numbers of the semispan model of a tailless airplane. Fins on; $\delta_a = 0^\circ$.

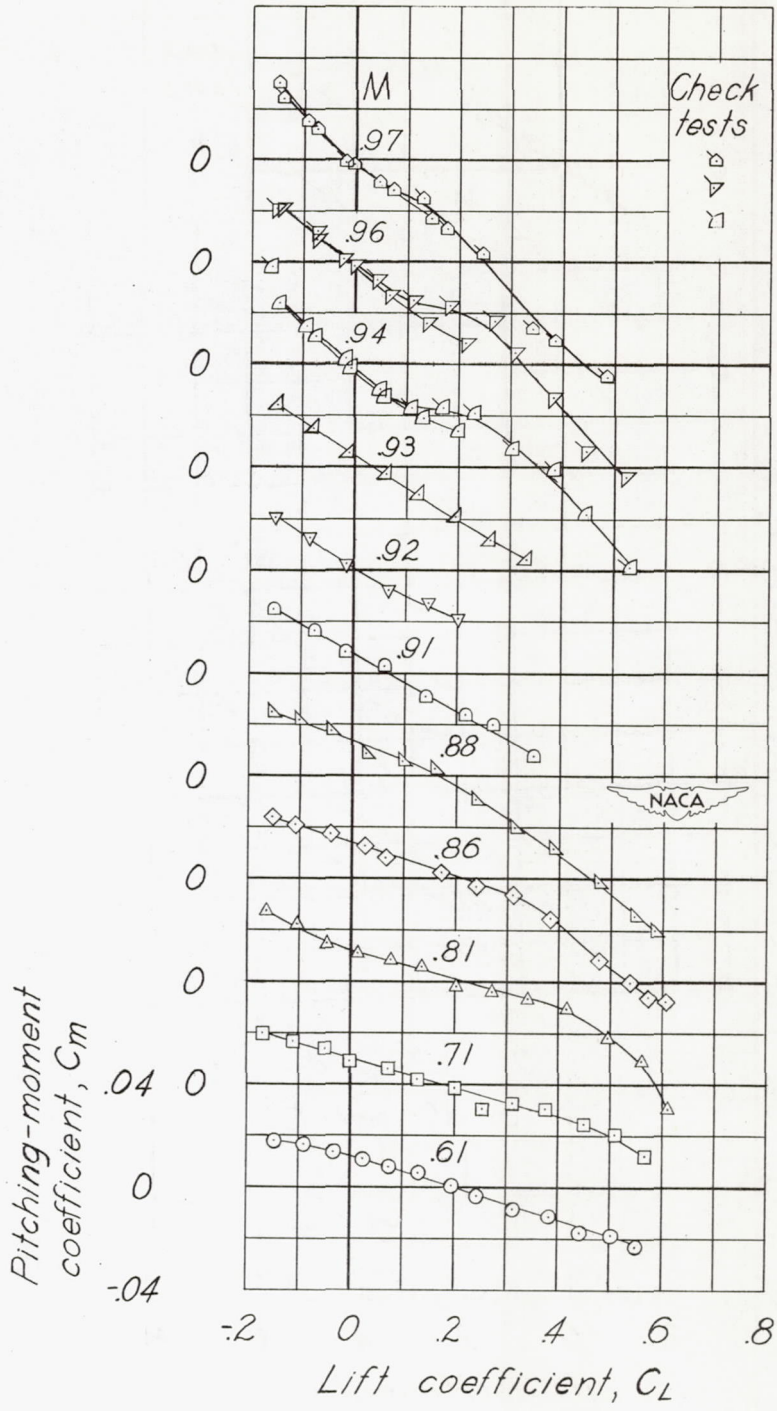

Figure 8.– Continued.

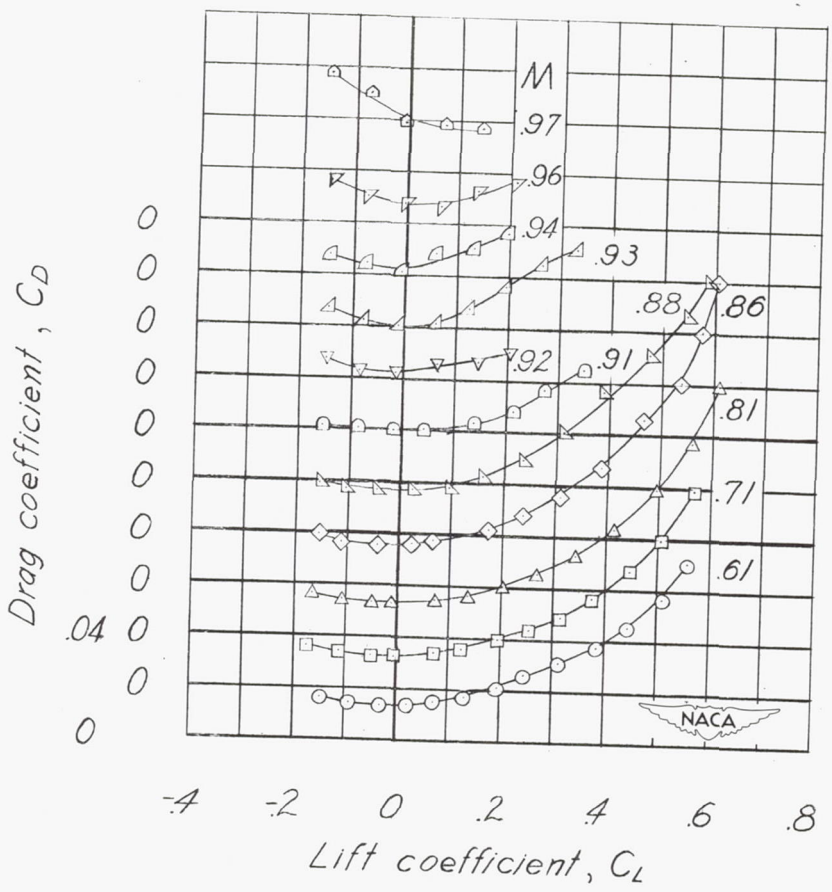

Figure 8.– Concluded.

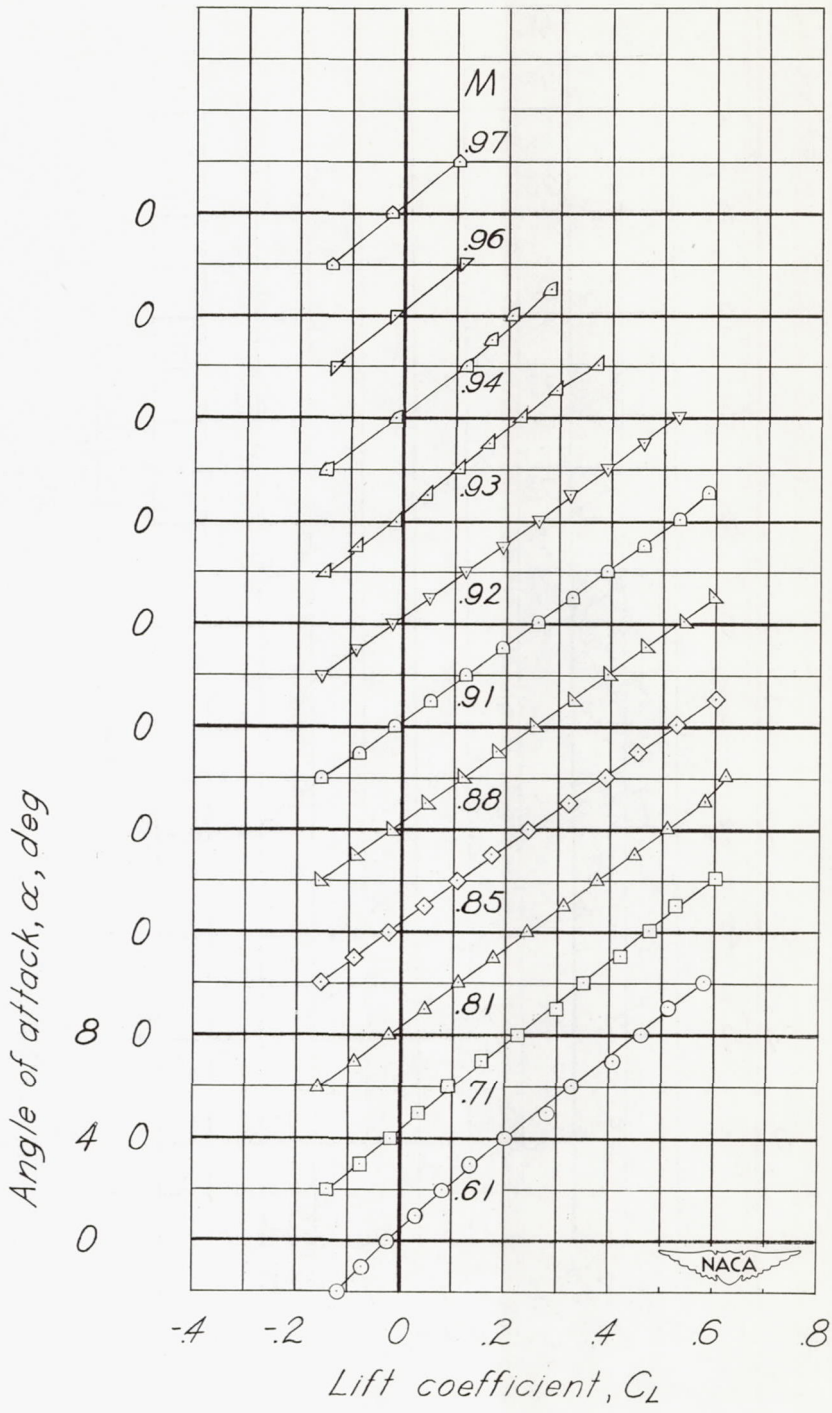

Figure 9.– Aerodynamic characteristics in pitch for various Mach numbers of the semispan model of a tailless airplane. Fins off; $\delta_a = 0^\circ$.

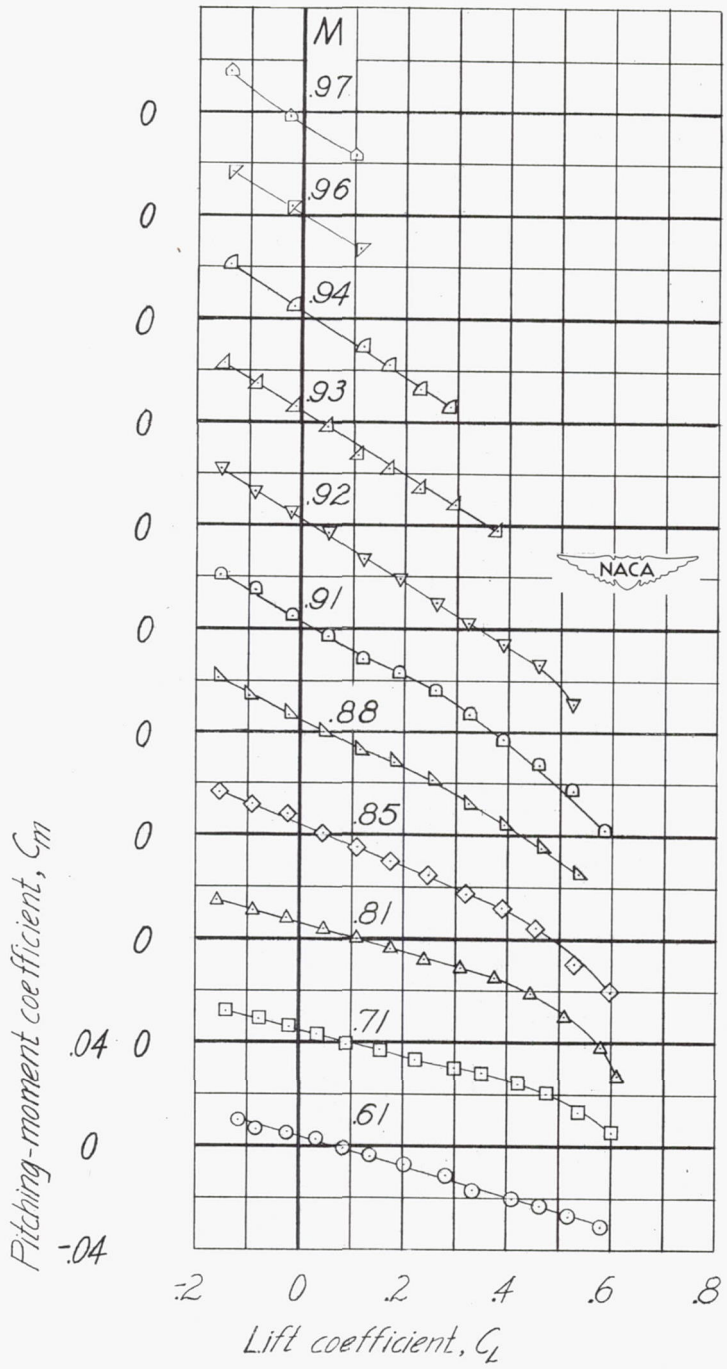

Figure 9.- Continued.

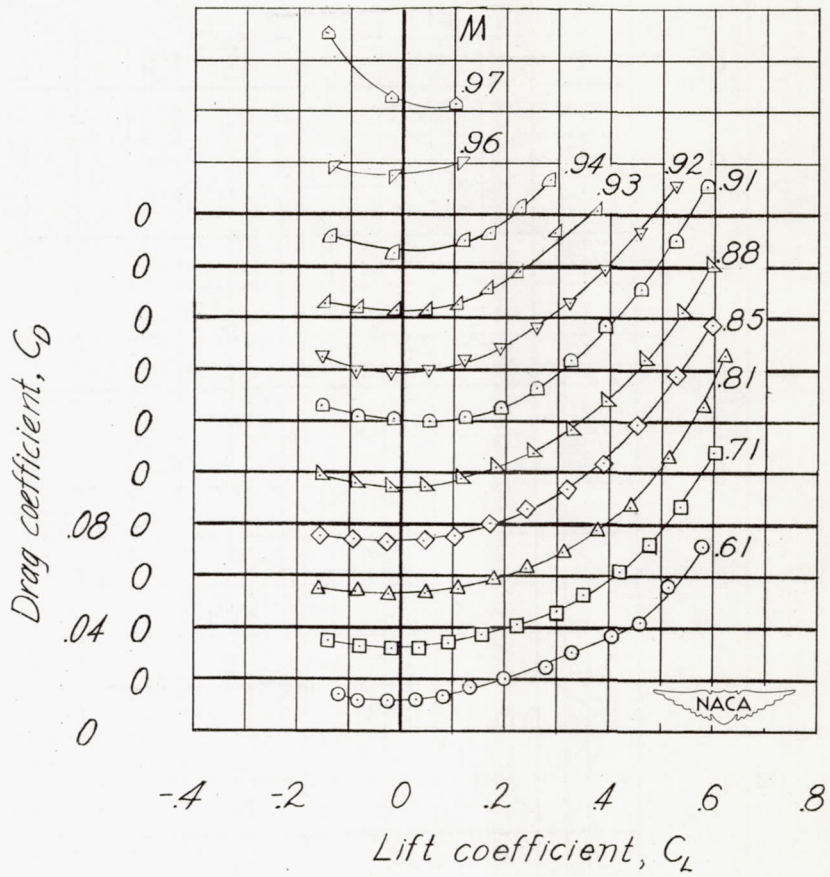

Figure 9.– Concluded.

Figure 10.– Effect of spoiler on aerodynamic characteristics for various Mach numbers of the semispan model of a tailless airplane. Fins on; $\delta_a = 0^\circ$.

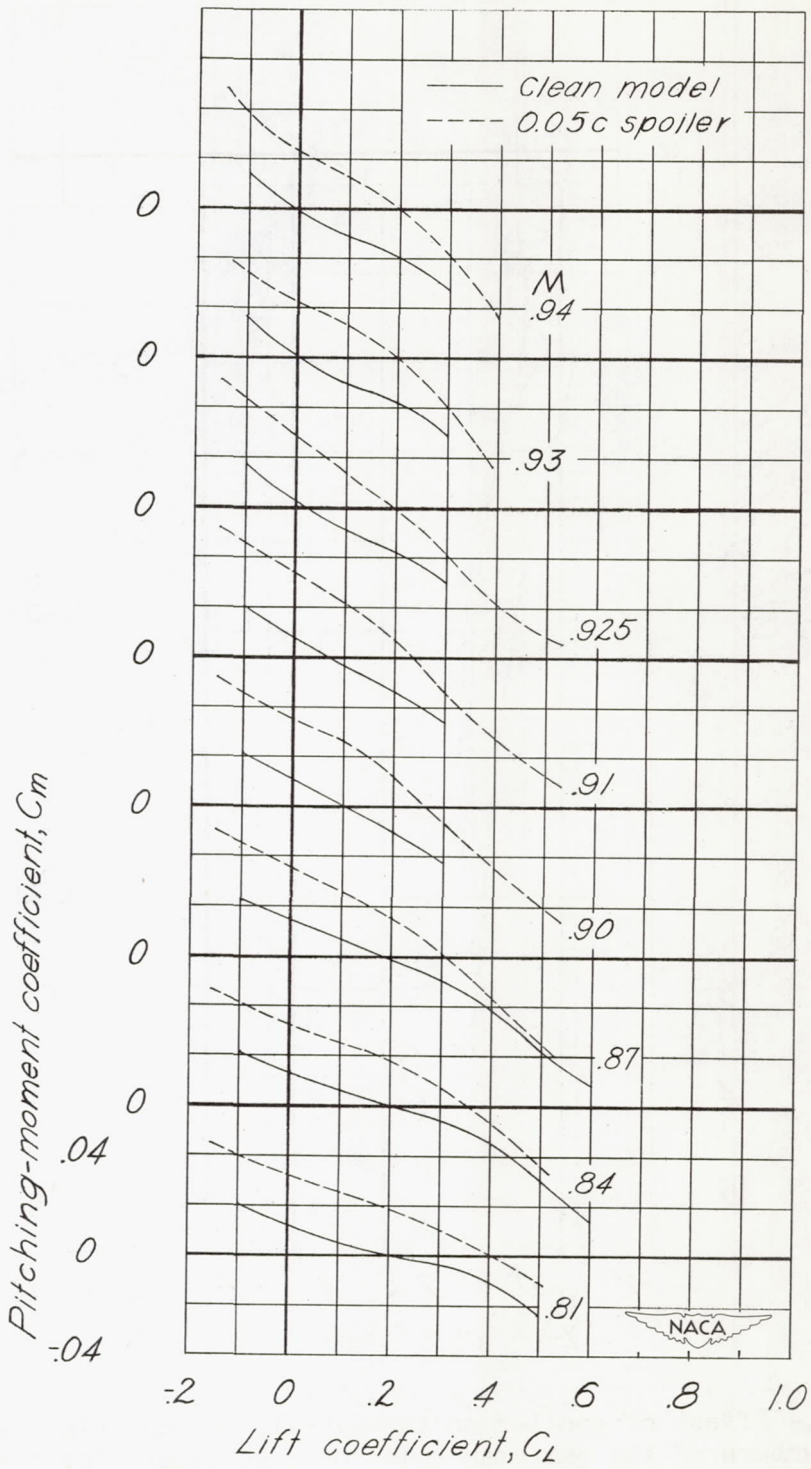

Figure 10.– Concluded.

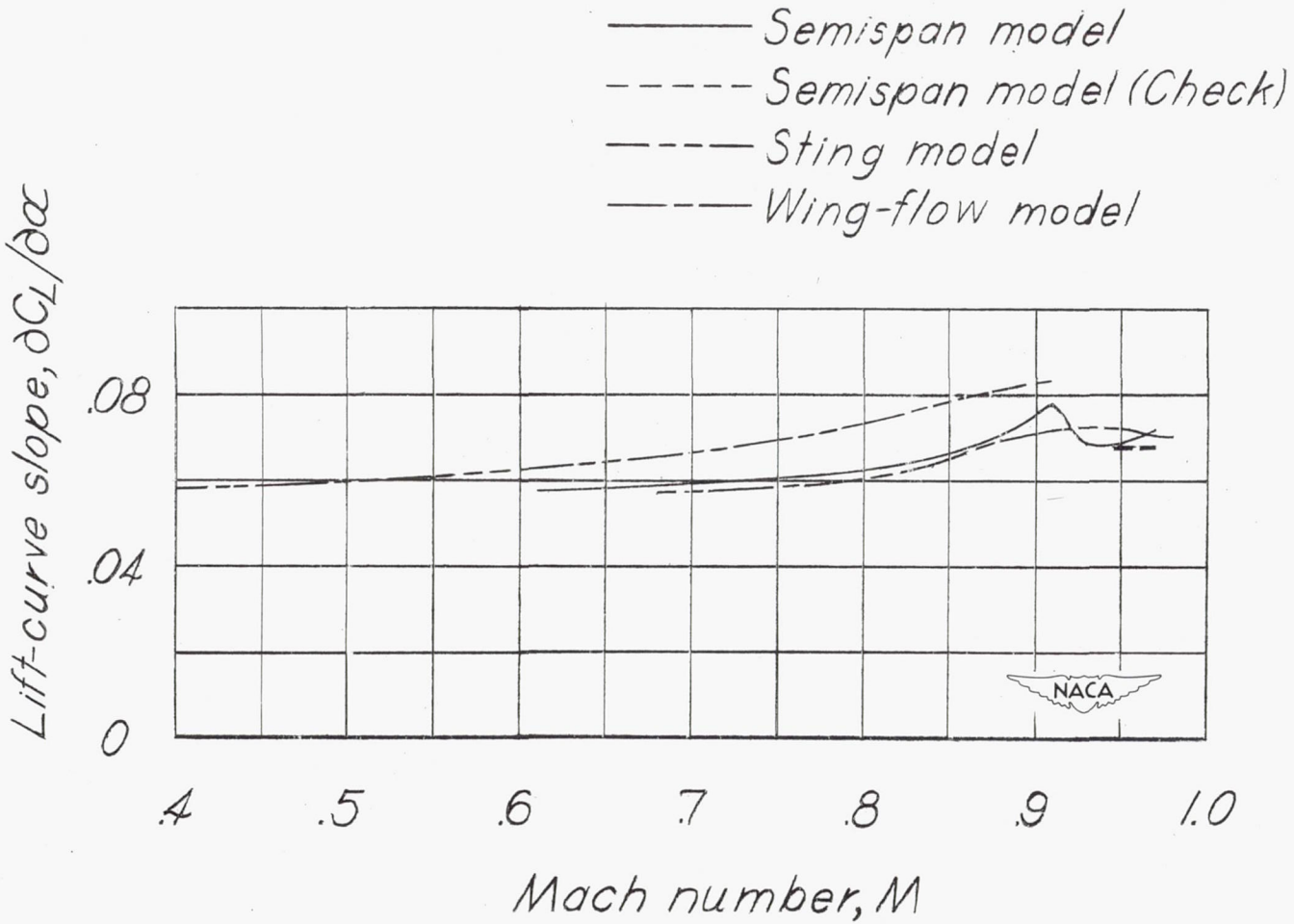

Figure 11.– A comparison of lift–curve slope variation with Mach number for the low–lift–coefficient range as obtained by three different test methods on models of a tailless airplane. Vertical fins on; $\delta_a = 0^\circ$.

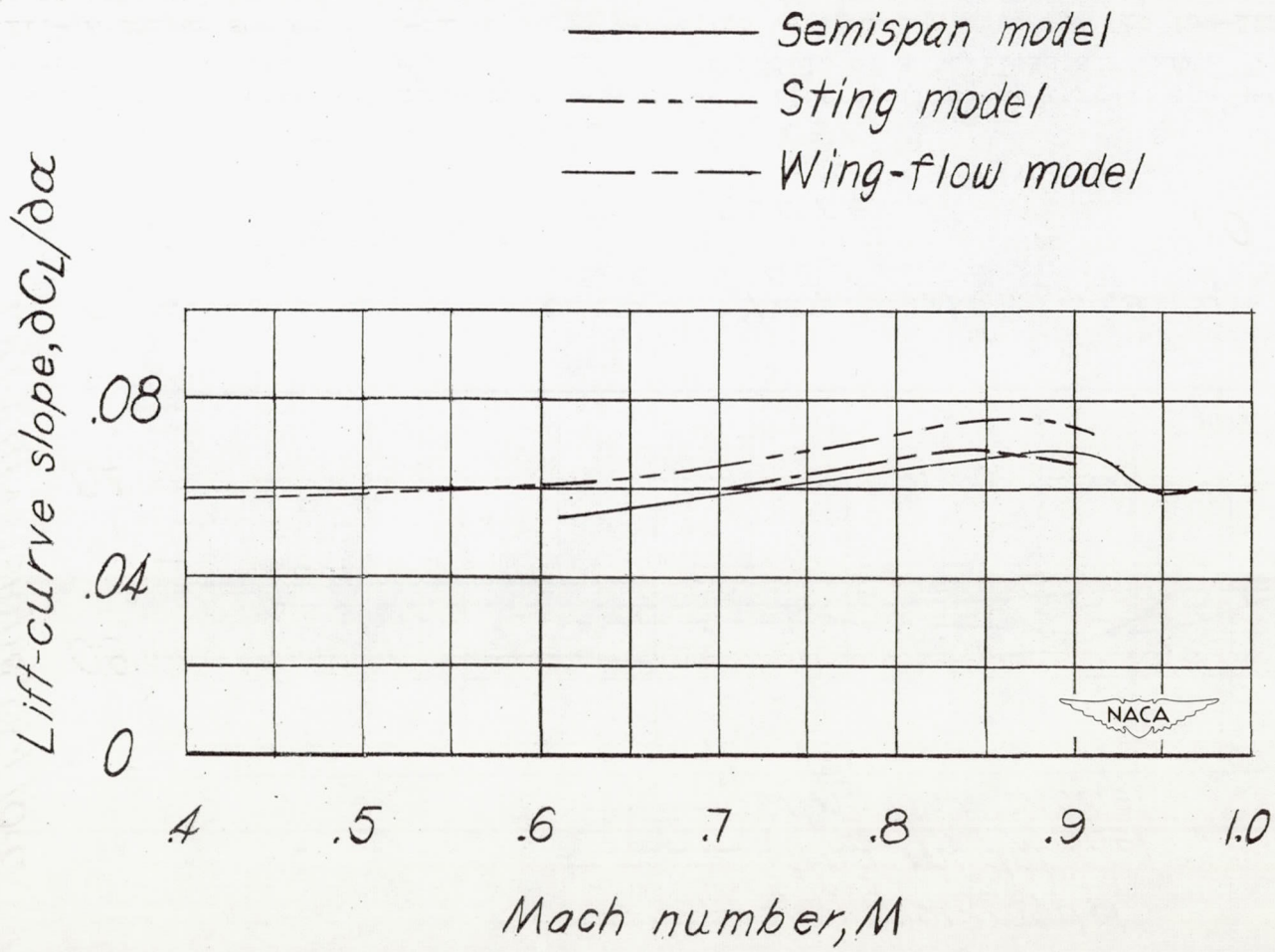

Figure 12.– A comparison of lift–curve slope variation with Mach number in the low–lift–coefficient range as obtained by three different test methods on models of a tailless airplane. Vertical fins off; $\delta_a = 0^\circ$.

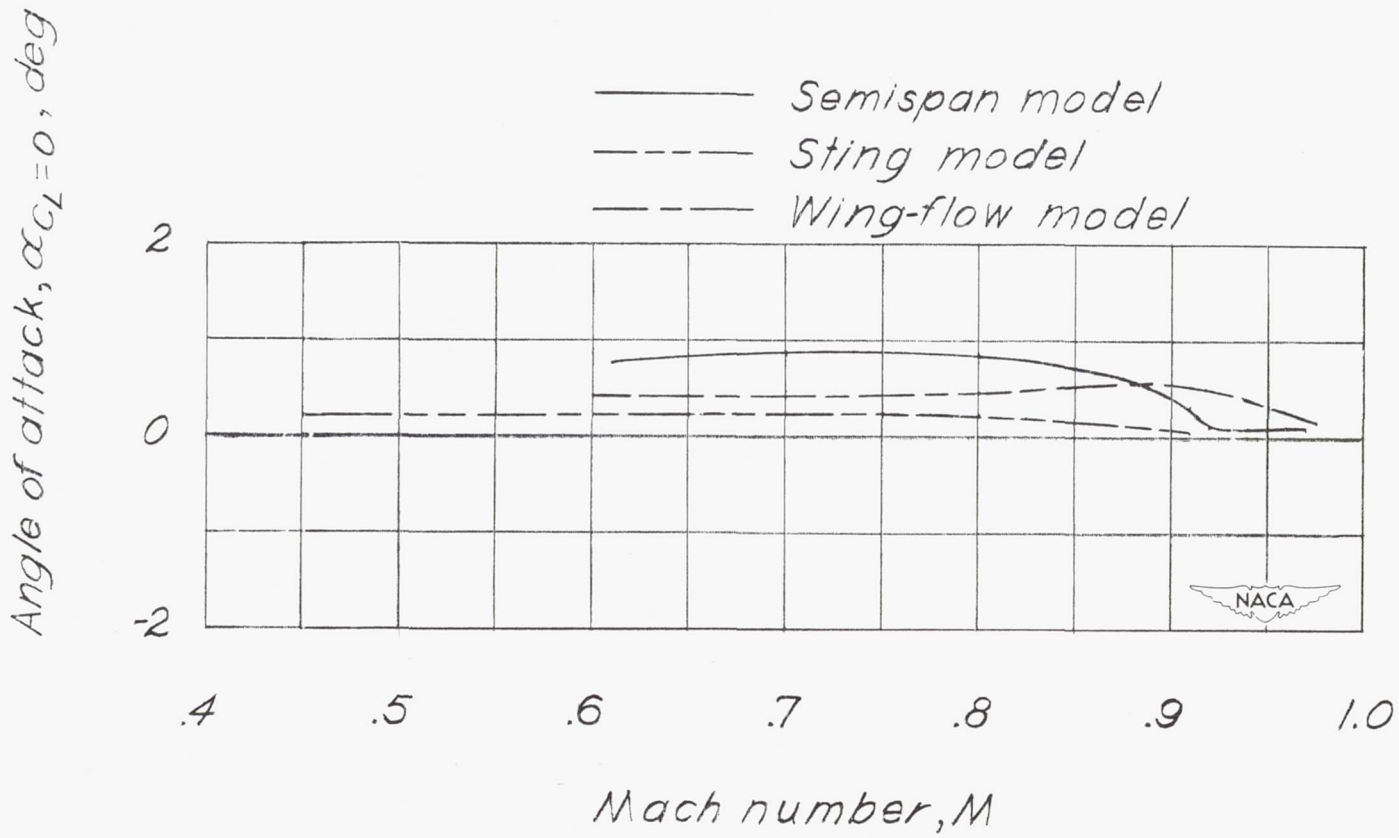

Figure 13.– A comparison of angle of attack at zero lift coefficient through the Mach number range as obtained by three different test methods on models of a tailless airplane. Vertical fins on; $\delta_a = 0^\circ$.

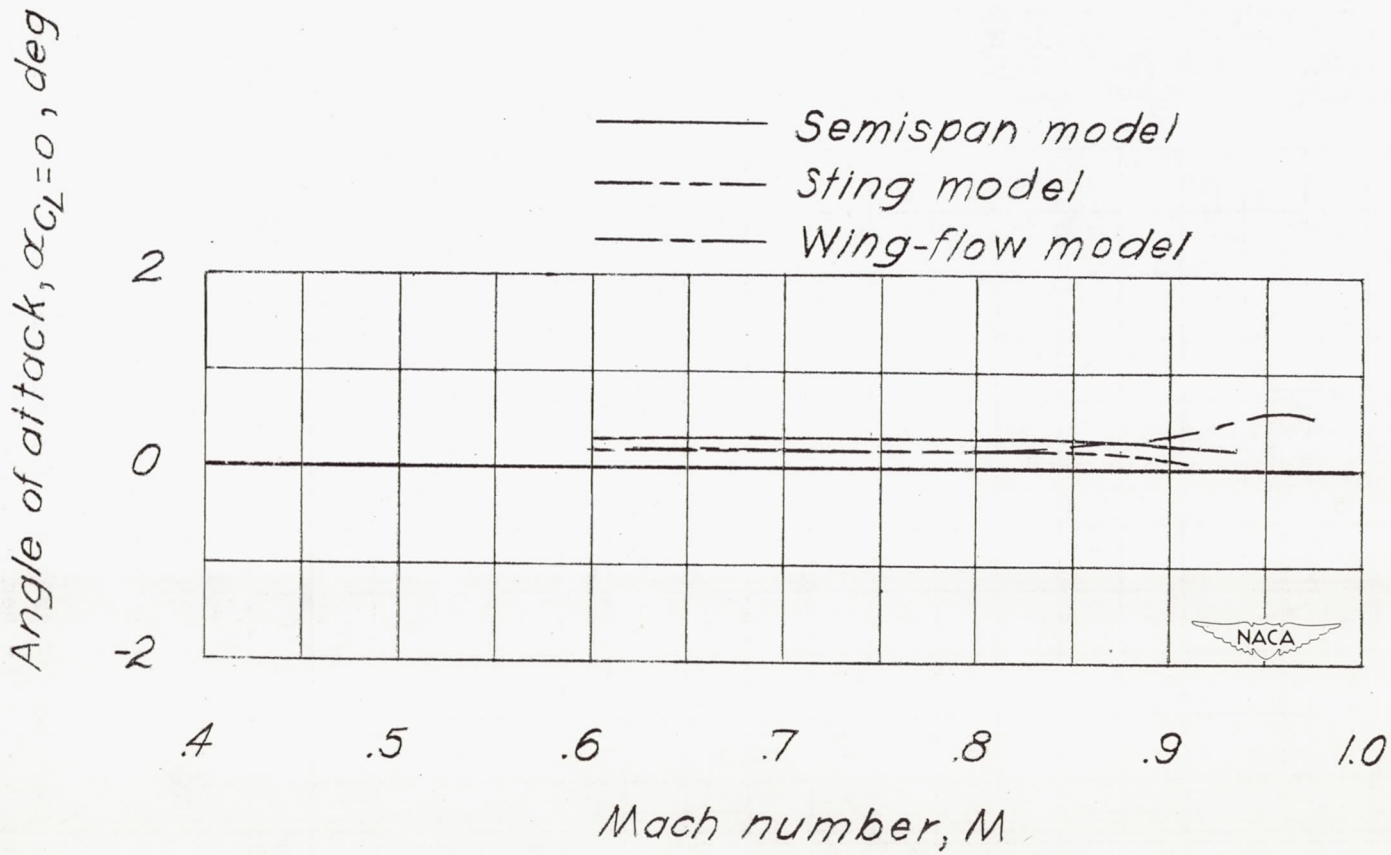

Figure 14.– A comparison of angle of attack at zero lift coefficient through the Mach number range as obtained by three different test methods on models of a tailless airplane. Vertical fins off; $\delta_a = 0^\circ$.

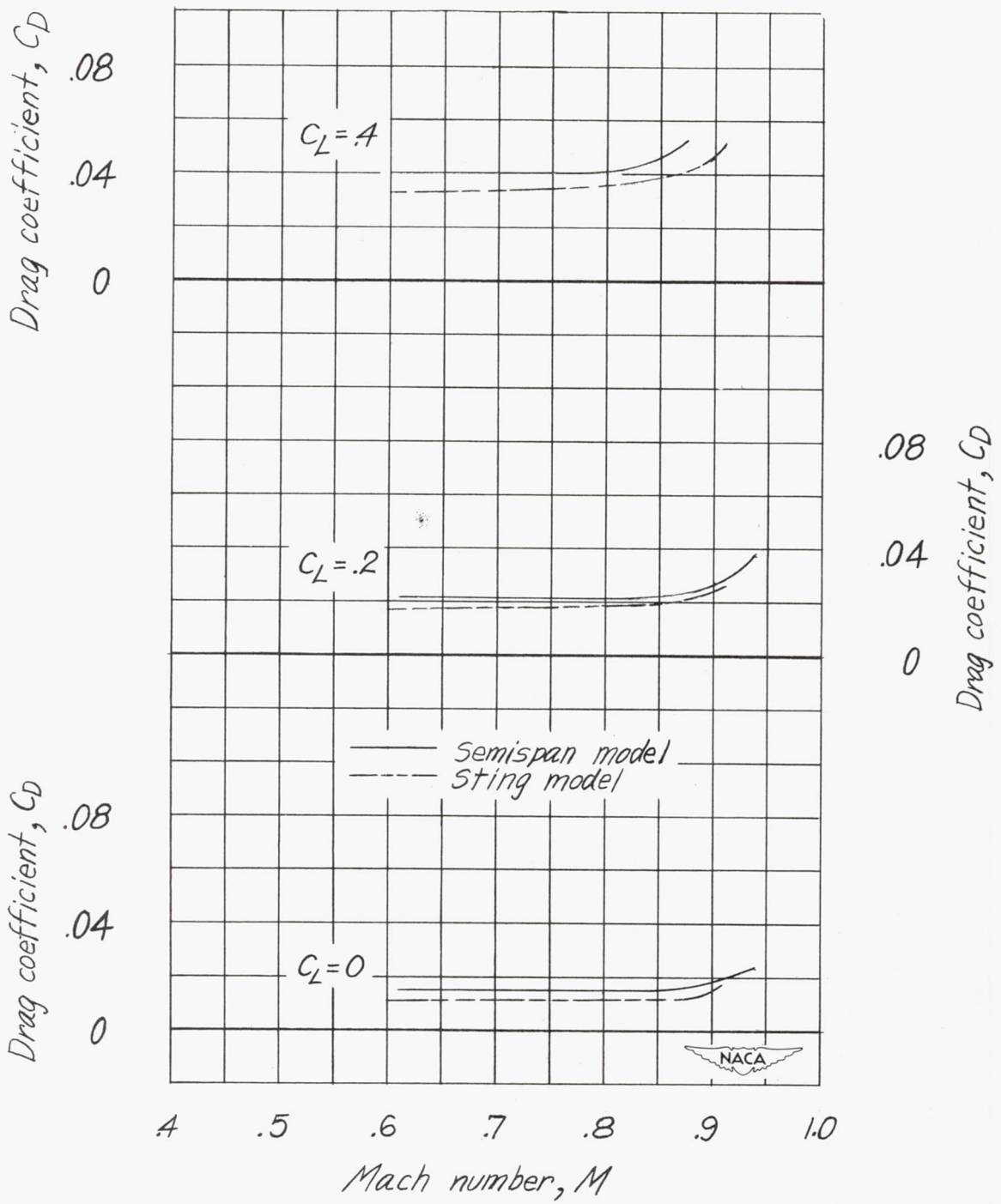

Figure 15.– A comparison of drag coefficient through the Mach number range as measured by the semispan and sting test methods on models of a tailless airplane. Vertical fins on; $\delta_a = 0^\circ$.

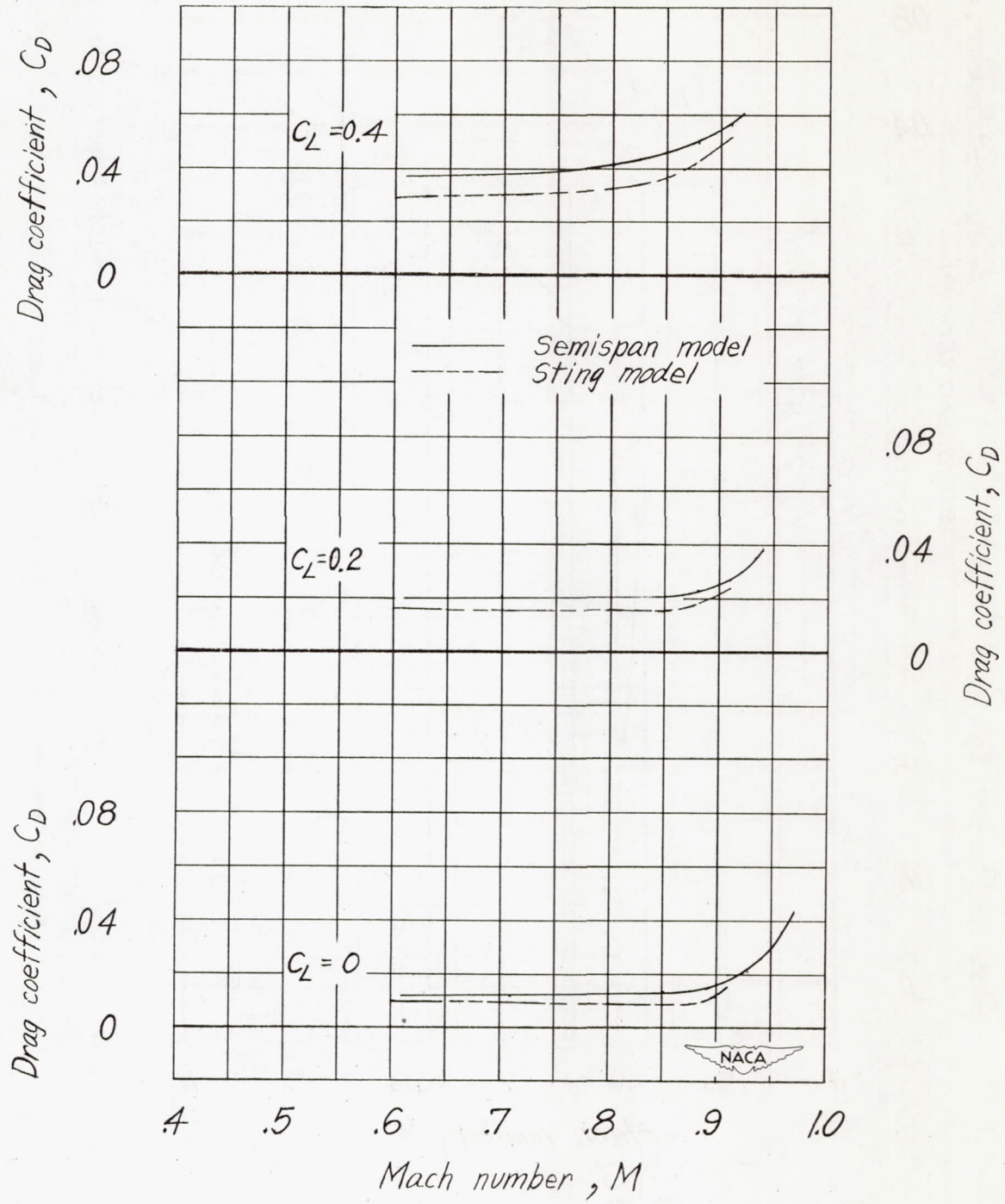

Figure 16.– A comparison of drag coefficient through the Mach number range as measured by the semispan and sting test methods on models of a tailless airplane. Vertical fins off; $\delta_a = 0^\circ$.

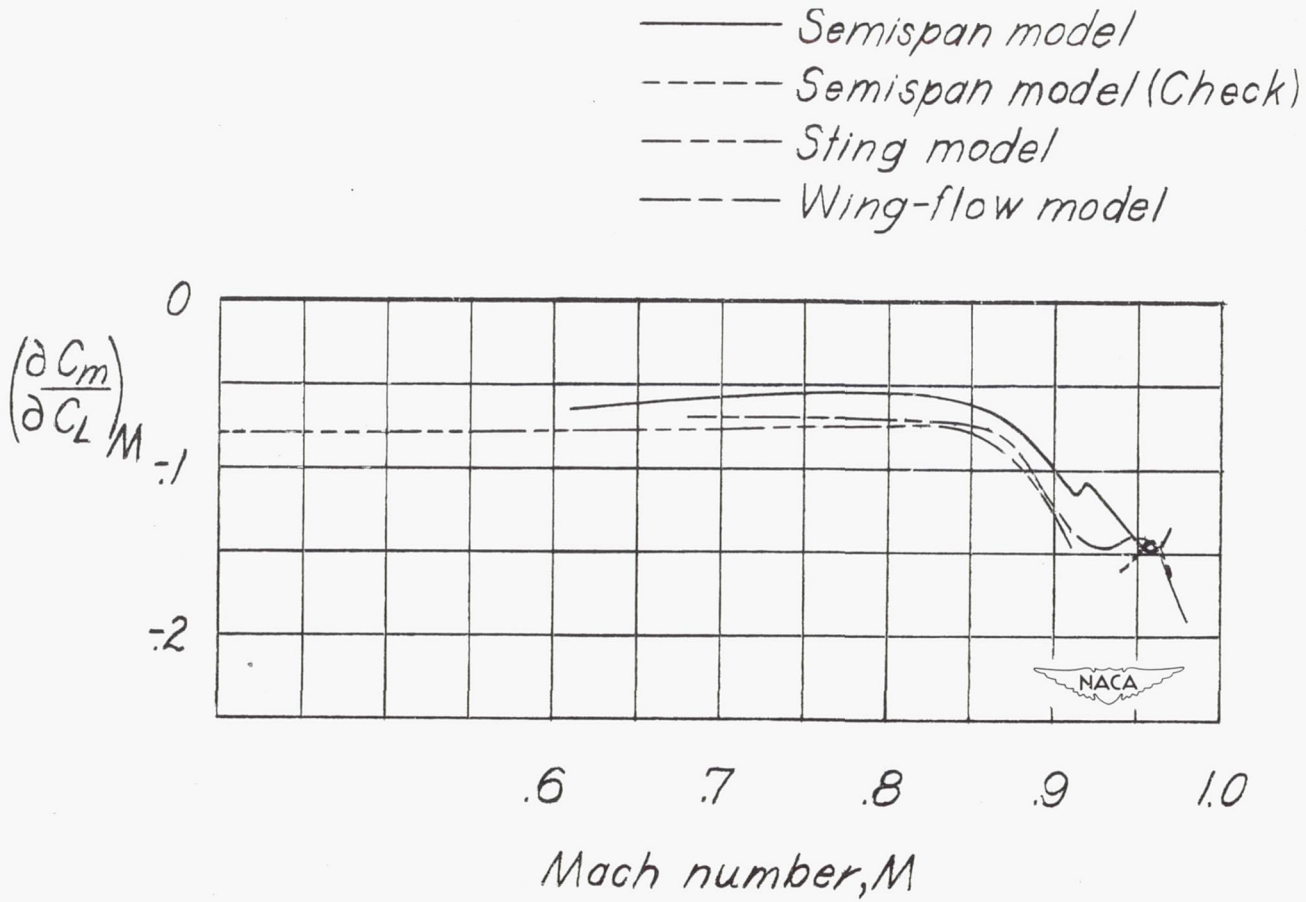

Figure 17.– A comparison of $\left(\frac{\partial C_m}{\partial C_L}\right)_M$ variation with Mach number for the low-lift-coefficient range as obtained by three different test methods on models of a tailless airplane. Vertical fins on; $\delta_a = 0^\circ$.

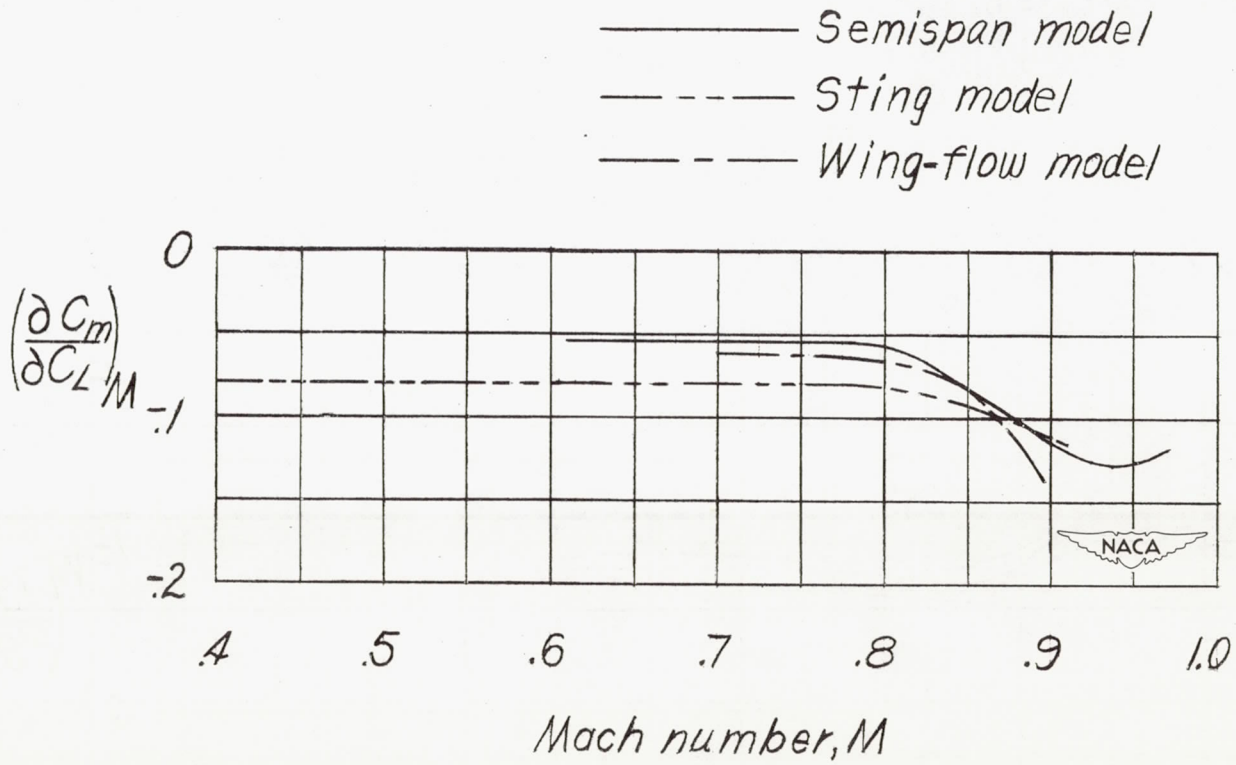

Figure 18.– A comparison of $\left(\frac{\partial C_m}{\partial C_L}\right)_M$ variation with Mach number for the low-lift-coefficient range as obtained by three different test methods on models of a tailless airplane. Vertical fins off; $\delta_a = 0^\circ$.

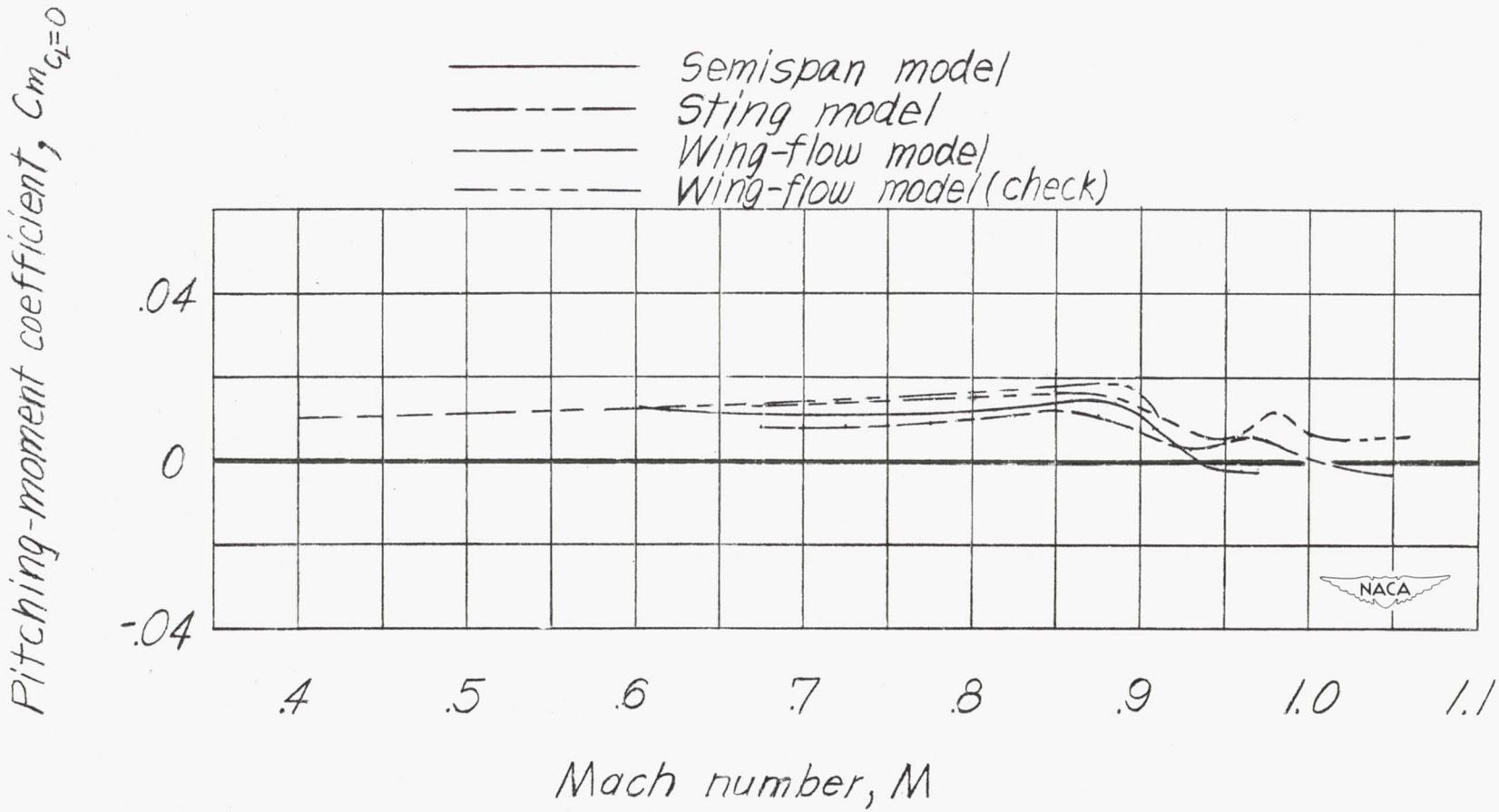

(a) Vertical fins on.

Figure 19.- A comparison of pitching-moment coefficient through the Mach number range at zero lift coefficient as obtained by different test methods on models of a tailless airplane. $\delta_a = 0^\circ$.

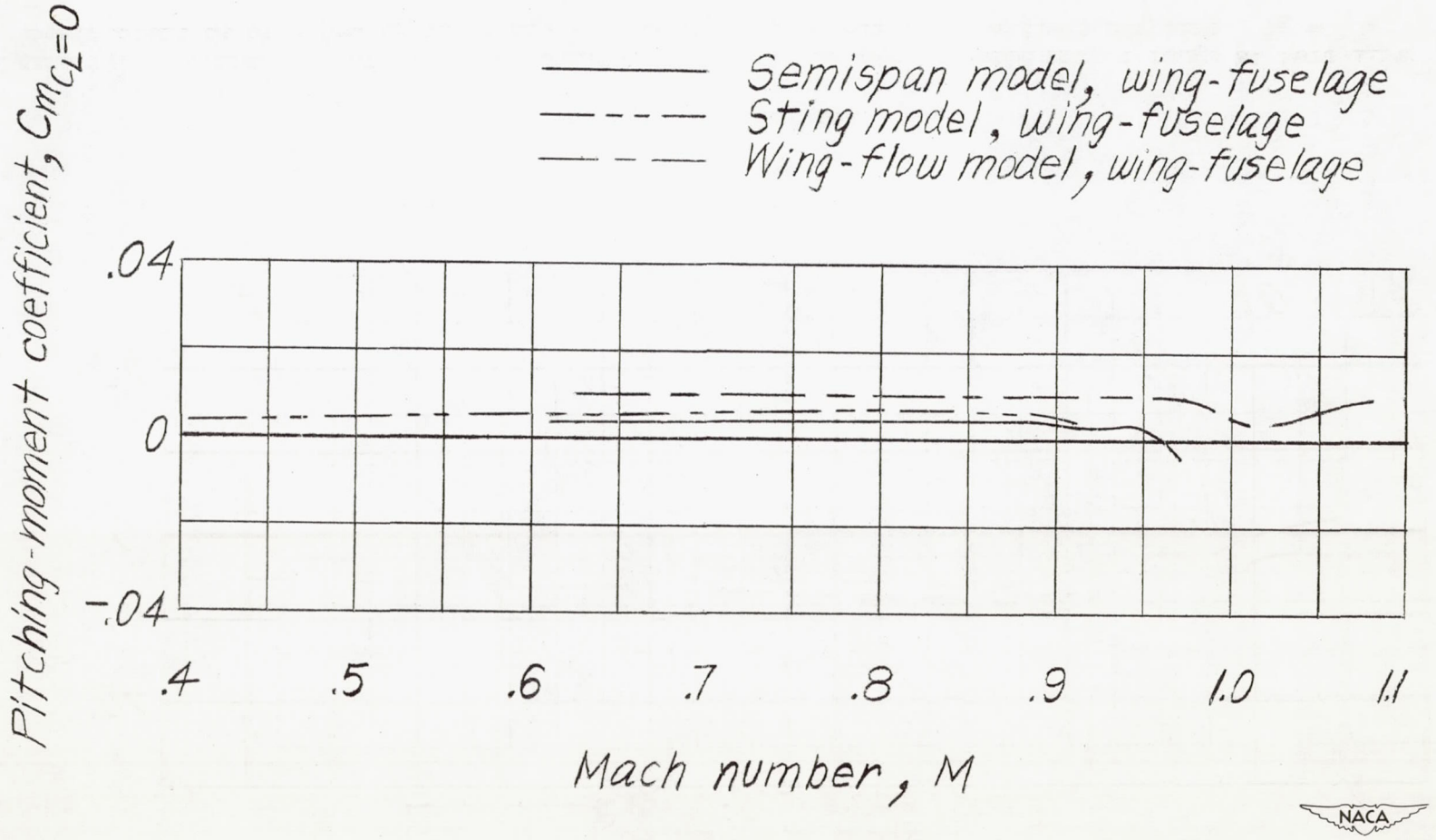

(b) Vertical fins off.

Figure 19.- Concluded.

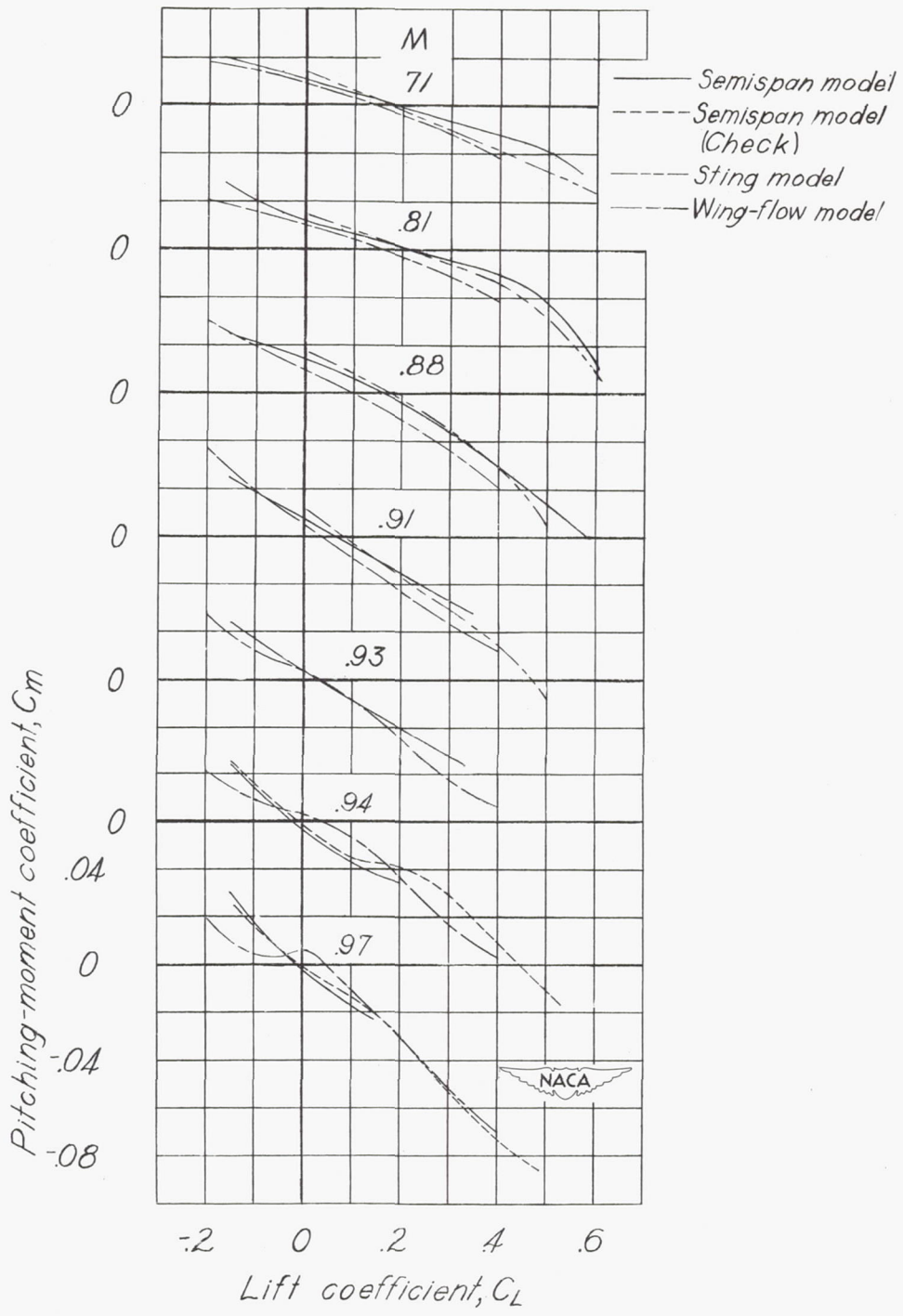

Figure 20.– A comparison of pitching–moment coefficients obtained by three different test methods on models of a tailless airplane. Vertical fins on; $\delta_a = 0^o$.

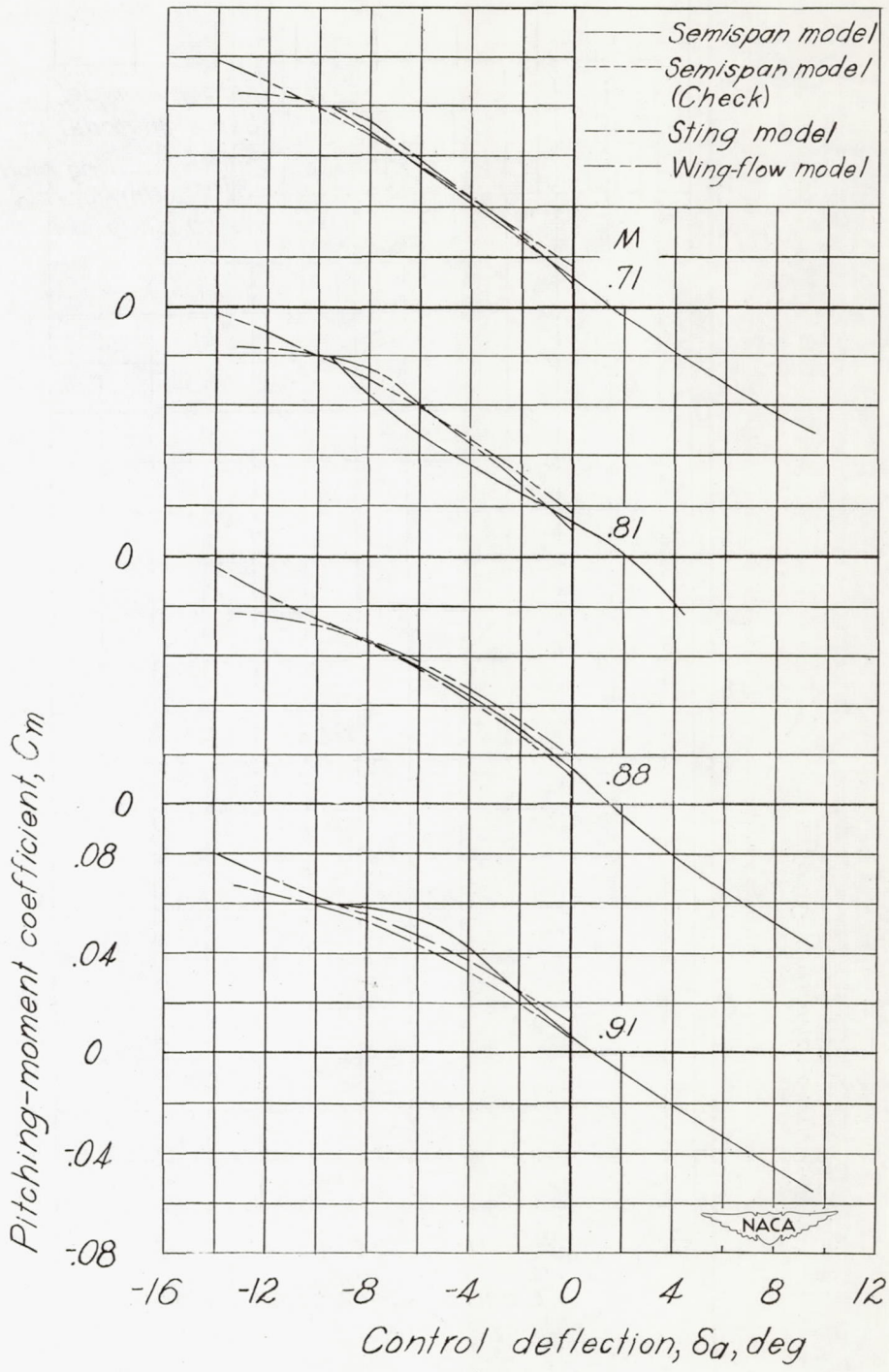

Figure 21.– A comparison of effectiveness for several Mach numbers as obtained by three different test methods on models of a tailless airplane. Vertical fins on; $C_L = 0$.

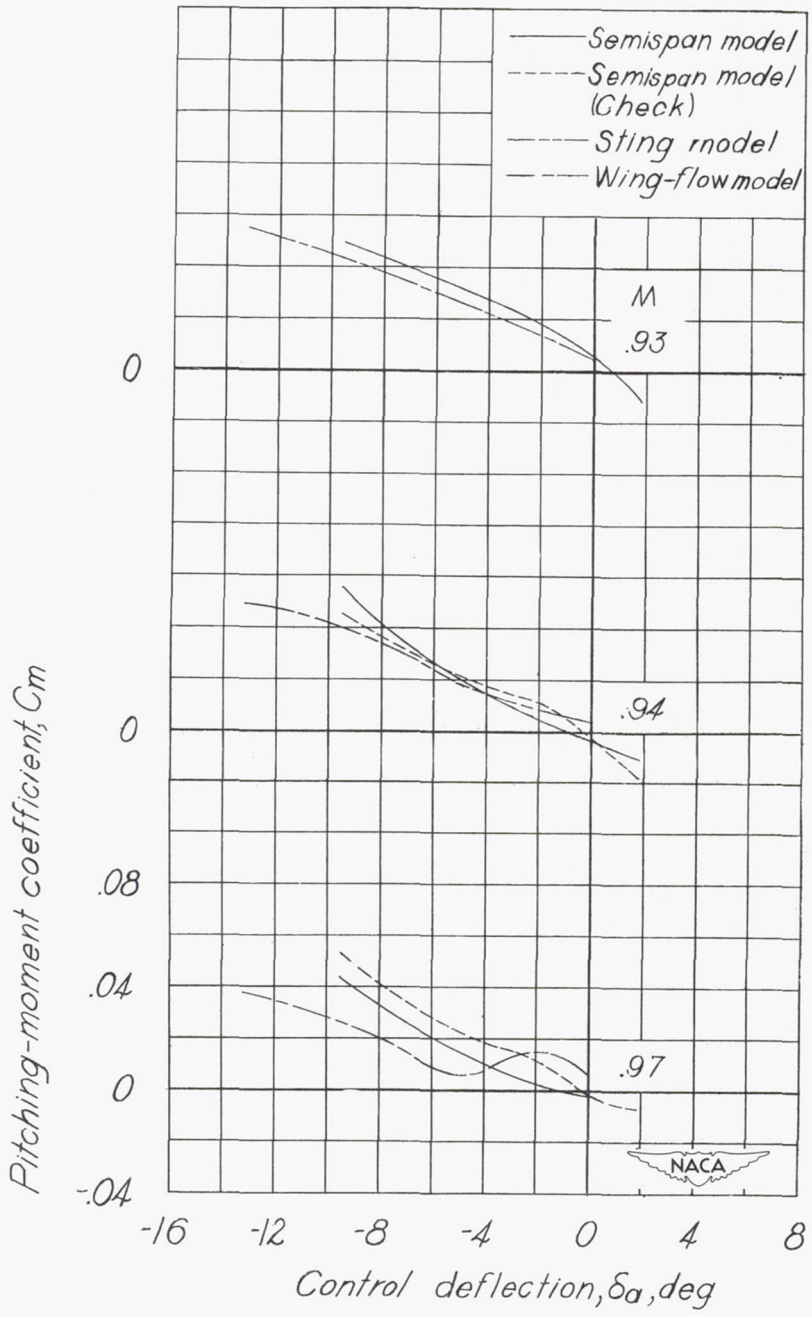

Figure 21.– Concluded.

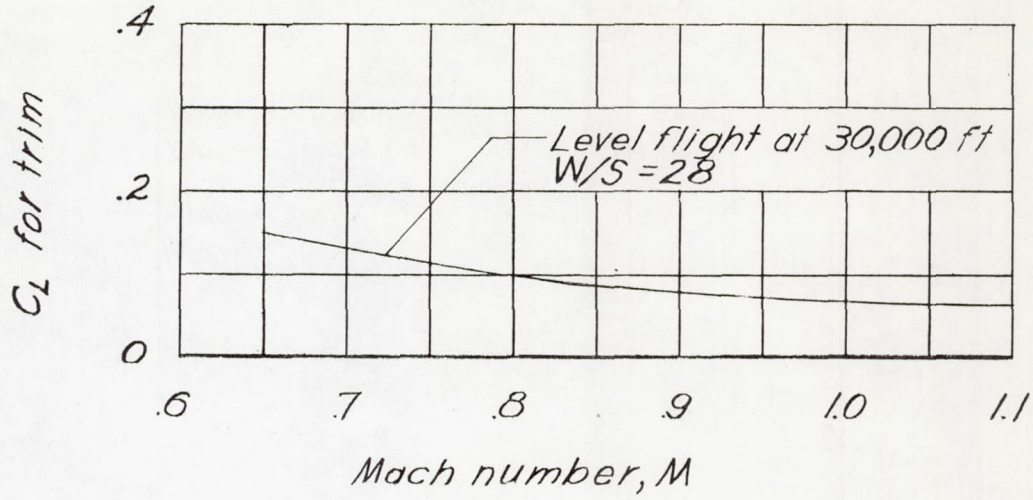

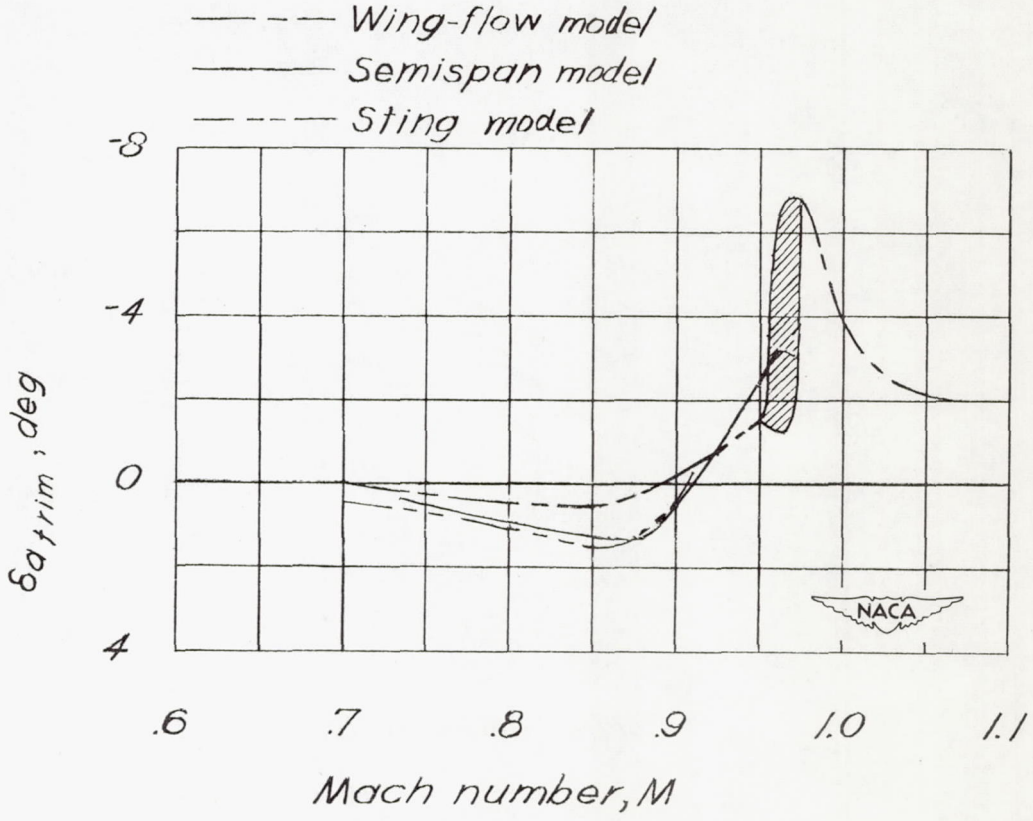

Figure 22.– Variation with Mach number of lift coefficient and control angle required for trim in level flight at an altitude of 30,000 feet with a wing loading of 28. Vertical fins on.